# The geology of Nevados de Chillán volcano, Chile

**Hugh J. Dixon**
**Mick D. Murphy**
**Steve J. Sparks**

Department of Earth Sciences, Bristol University, Wills Memorial Building, Bristol BS8 1RJ, U.K.
e-mail: steve.sparks@bristol.ac.uk

**Rodrigo Chávez**
**José A. Naranjo**

Servicio Nacional de Geología y Minería, 0104, Avenida Santa María, Santiago, Chile
e-mail: jnaranjo@sernageomin.cl

**Peter N. Dunkley**
**Simon R. Young**

British Geological Survey, Keyworth, Nottingham NG12 5GG, U.K.

**Jennie S. Gilbert**

Environmental Geosciences Division, Lancaster University, Lancaster LA1 4YQ, U.K.

**Malcolm R. Pringle**

Scottish Universities Research Reactor Centre, East Kilbride, Glasgow G75 0QF, U.K.

## ABSTRACT

Nevados de Chillán volcano is a large composite stratovolcanic complex in the Southern Volcanic Zone of the Chilean Andes. It is one of the highest-risk volcanoes in Chile due to high levels of historic activity and rapid development of economic activity in the area. High precision $^{40}Ar/^{39}Ar$ and $^{14}C$ geochronology, geochemistry and petrology have been employed in addition to photogeology and field mapping to elucidate the evolution of this volcano and assess its hazards. Nevados de Chillán has been active since at least 640 ka when a large group of subglacial andesite flows were erupted. Since 100 ka, sequences of andesite and dacite lavas have been erupted into both subaerial and subglacial environments. Ignimbrites were erupted at around 40 ka and may have been associated with caldera collapses. Two separate eruptive centres have evolved since 40 ka: the Cerro Blanco and Las Termas subcomplexes. The two centres are 6 km apart, yet have contemporaneously erupted geochemically distinct magmas. Subglacial lavas have been identified on the high flanks of the volcano and $^{40}Ar/^{39}Ar$ dating has confirmed their eruption during recent glaciations (isotope stages 4 and 2). Tephra fall deposits have been dated by $^{14}C$ analysis of interstratified organic material and indicate that no proximal tephra fallout deposits older than 9 ka remain. Tephra dispersal indicates that Holocene activity has involved vulcanian to subplinian eruptions. At least, 3 pyroclastic flow eruptions have occurred during the Holocene and lahar deposits are common in the valleys around the volcano. Historically, the Santa Gertrudis vent erupted during 1861-1865 and the dacite lava cone complexes Nuevo and Arrau were constructed during 1906-1943 and 1973-1986, respectively. Historic records indicate that lahars and landslides are major hazards to economic developments on the lower flanks and valleys

*Key words: Subglacial volcanism, Volcanic hazards, $^{40}Ar/^{39}Ar$, Geochronology, Southern Volcanic Zone, Nevados de Chillán, Andes.*

*Revista Geológica de Chile, Vol. 26, No. 2, p. 227-253, 3 tables, 17 Figs., December 1999.*

## RESUMEN

**La geología del volcán Nevados de Chillán, Chile.** El Nevado de Chillán es un complejo estratovolcánico compuesto, ubicado en la Zona Volcánica Sur de los Andes. Debido al rápido desarrollo de la actividad económica en el área y a la frecuencia de la actividad eruptiva histórica, es uno de los volcanes de más alto riesgo de Chile. Junto con la realización de estudios fotogeológicos y mapeo de terreno se han empleado técnicas geocronológicas ($^{40}Ar/^{39}Ar$, $^{14}C$), geoquímicas y consideraciones petrológicas para elucidar la evolución del volcán. El Nevado de Chillán ha estado activo desde, a lo menos, 640 ka, a partir de la emisión de un gran volumen de lavas subglaciales. Desde los 100 ka han sido eruptadas lavas dacíticas y andesíticas en ambientes subaéreos y subglaciales. Alrededor de los 40 ka fueron eruptadas ignimbritas que pudieron asociarse con el colapso de calderas, generándose abruptos escarpes hacia el interior de las mismas, alrededor del volcán. Desde los 40 ka han evolucionado dos centros eruptivos separados: los subcomplejos Cerro Blanco y Las Termas. Estos centros, distantes seis km en dirección noroeste han eruptado, en forma contemporánea, magmas geoquímicamente distintos. Se han identificado lavas subglaciales en las partes altas del volcán, las cuales han sido datadas mediante $^{40}Ar/^{39}Ar$, confirmando que se produjeron durante las glaciaciones recientes (estadios isotópicos 4 y 2). Los depósitos de caída de tefra han sido datados mediante análisis de $^{14}C$, de materiales orgánicos interestratificados, comprobándose que no existen remanentes de caída de tefra proximales más antiguos que 9 ka. La dispersión de la tefra indica que la actividad holocena incluye erupciones del tipo vulcaniano a subpliniano. Además, han ocurrido, a lo menos, 3 erupciones de flujos piroclásticos durante el Holoceno y los depósitos laháricos son de común ocurrencia en los valles de alrededor del volcán. Históricamente, se distinguen los centros Santa Gertrudis, que hizo erupción durante 1861-1865, y los complejos de conos de lavas dacíticas llamados Nuevo y Arrau, construidos durante 1906-1943 y 1973-1986, respectivamente. Los registros históricos indican que los lahares y deslizamientos son los mayores peligros para el desarrollo económico de los sectores sobre la parte baja de los flancos y valles.


*Palabras claves: Volcanismo subglacial, Peligros volcánicos, $^{40}Ar/^{39}Ar$, Geocronología, Zona Volcánica Sur, Nevados de Chillán, Andes.*

## INTRODUCTION

Nevados de Chillán volcano lies in the Southern Volcanic Zone of the Andean Cordillera at 36°50'S, 71°25'W (Fig. 1). Nevados de Chillán is a large composite stratovolcano constructed on a basement of granitic intrusive rocks and Cenozoic lavas. The main vents of the volcano extend along a 10 km long northwest trending ridge. The young parts of the volcanic edifice and associated lavas are divided into two subcomplexes about 6 km apart: the predominantly andesitic Cerro Blanco (CB) subcomplex and the more silicic Las Termas (LT) subcomplex (Fig. 2),separated by a saddle region. Satellite cones in the saddle can be assigned to the appropriate subcomplex by geochemistry. There are also extensive older lavas (Fig. 1), and pyroclastic deposits which predate much of the edifice and infill many of the valleys around the volcano. These older units cannot be definitely assigned to either subcomplex. Previous work at the volcano (Déruelle and Déruelle 1974) also proposed the division into two centres and interpreted inward facing scarps on the southern and western sides of the complex as remnants of caldera walls. The compositional range at Nevados de Chillán is from basaltic andesite to low-silica rhyolite [53-71% $SiO_2$]. A striking feature of the volcanic sequence is the alternation of subglacial and subaerial volcanic rocks, indicating an extensive history spanning interglacial and glacial periods.

This study extends the understanding of the distribution of eruptive products and the chronology of historical and earlier activity. The geological assessment combined photogeological interpretation, field mapping and stratigraphy, geochemistry and petrology, geomorphology, and radiocarbon and $^{40}Ar/^{39}Ar$ geochronology. This study was carried out primarily as part of a hazards assessment (J.S. Gilbert)[1]. Nevados de Chillán volcano is one of the highest risk volcanoes in Chile. The south-western flanks are being rapidly developed with tourist facilities for winter sports and summer vacations. This is in addition to the existing agricultural and logging activities in the area. The most recent activity (1906-1943 and 1973-1986) produced potentially unstable

1998. Volcanic hazards at volcán Nevados de Chillán (Unpublished), *British Geological Survey*, 36 p. Keyworth, Nottingham, U.K.

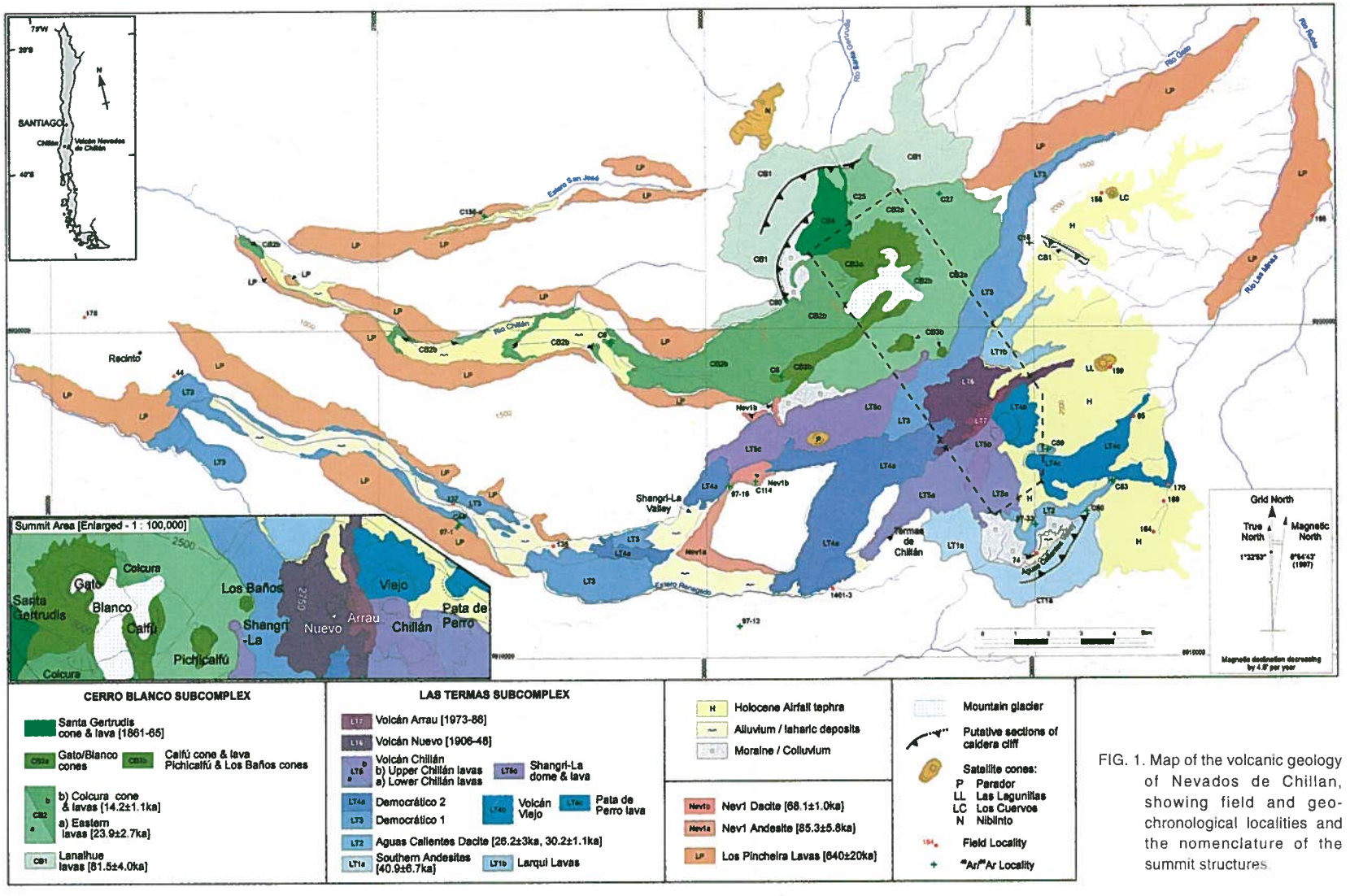


FIG. 1. Map of the volcanic geology of Nevados de Chillan, showing field and geochronological localities and the nomenclature of the summit structures.

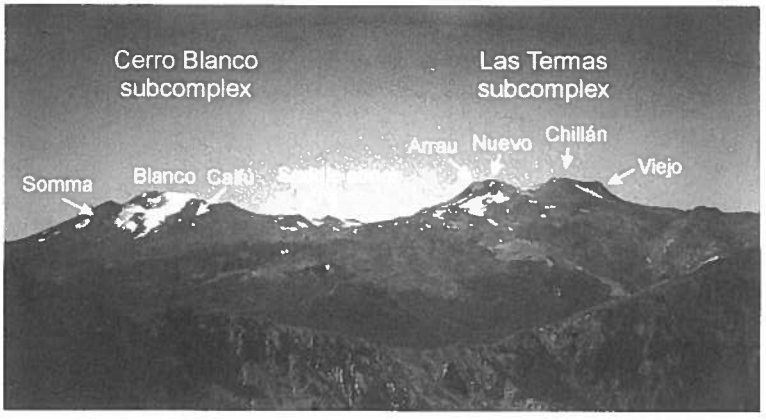


FIG. 2. Nevados de Chillan volcanic complex from the south-west showing main cones and structures.

coulée lava cones located directly above extensive skiing facilities. Holocene pyroclastic flow and tephra-fall deposits have been identified around the volcano. Lahar deposits occur in river valleys and historical records indicate that eruptions in 1861-1865 produced major lahars to the north and north-east of the volcano due to snow-melt.

The paper is organised as follows:

First, the new reconnaissance geological map and outline stratigraphy are described; second, new geochronological data are presented; third, the basic petrological and geochemical characteristics of the volcano are described with comments on the use of geochemistry for correlation of stratigraphic units. The geology is, then, documented in detail, and finally, the new information is discussed with emphasis on the evolution of the complex, and the alternation of interglacial and glacial age volcanic rocks.

## MAPPING AND STRATIGRAPHY

This account of the geology of the Nevados de Chillán volcanic system is based on a reconnaissance geological study together with new geochronological data and with reference to new petrological and geochemical data (M.D. Murphy[2]; M.D. Murphy[3]). The volcano has been divided up into units which are based primarily on whether they represent mappable units rather than on strictly stratigraphic criteria; a formalised stratigraphic division proved unworkable. In addition to field mapping, new $^{14}C$ and $^{40}Ar/^{39}Ar$ ages and use of geochemical and petrological data have confirmed and, in some cases, demonstrated stratigraphic correlations.

The geological map (Fig.1) shows the distribution of the main stratigraphic units. Access limitations mean that the detail of mapping of the las Termas (LT) subcomplex is significantly greater than that of the Cerro Blanco (CB) subcomplex. More detailed mapping would reveal more complexity in the earlier history of the volcano. The units are not, in general, of equal status because the definition of meaningful units has much higher resolution in the youngest products of the volcano. Furthermore, the stratigraphic relationships between some units are either not known or are based on insufficient data. The units are presented in the best interpretation of stratigraphic order, but should be seen as mappable units only, with ambiguity in some cases with regard to relative ages.

The Los Pincheira unit is a major group of subglacial andesite lavas that form spectacular 100-200 m thick valley-side benches. The Nev1a and 1b lavas are examples of pre-subcomplex lavas

[2] 1995. The geology and geochemistry of Nevados de Chillán volcano, Chile (Unpublished), *British Geological Survey*, p. 188. Keyworth, Nottingham, U.K.

[3] 1995. The geology and geochemistry of Nevados de Chillán volcano, Chile - Second Report (Unpublished), *British Geological Survey*, p. 147. Keyworth, Nottingham, U.K.

mapped in some detail as they are located in the (accessible) Shangri-La valley. The Nev1b dacite contains remarkable examples of columnar-jointing due to ice-chilling. The Nev2 Pleistocene ignimbrites are widely distributed to the west of the volcano. The ignimbrite distribution was not mapped in detail and has therefore been omitted from figure 1.

The CB subcomplex was mapped in limited detail due to the remoteness of much of the northern and eastern area combined with extensive moraine and colluvium cover preventing detailed photo-interpretation. Sectors of inward-facing arcuate cliffs cut the oldest units of each subcomplex (CB1 and LT1a lavas) and could be interpreted as sections of caldera walls. The lava formations are geochemically distinct, but both are subaerial andesites dipping shallowly away from the centre of the volcano. The putative caldera collapse event(s) may be associated with the Nev2 ignimbrites.

Within the CB subcomplex, CB2a and CB2b are somewhat crude groupings based on geochemistry and distribution. An early shield-volcano phase was followed by the construction of a stratocone which subsequently underwent sector collapse and major glacial erosion. The remnants underlie the postglacial CB3a (Gato and Blanco) and CB3b (Calfú) cones (Fig. 1). The Pichicalfú and Los Baños cones in the saddle region were geochemically correlated with CB3b. The CB4 Santa Gertrudis lava was erupted in 1861-1865 from a flank vent and is compositionally equivalent to the CB3b Calfú group. The most recent tephra fall (Hc) on the eastern and north-eastern flanks is also geochemically identical to CB3b/CB4.

The LT subcomplex comprises overlapping post-glacial cones and craters, and associated dacite and andesite lavas that reach up to 35 km down the valleys surrounding the volcano. The LT1b Larqui lavas are a probable remnant block of the earliest Las Termas structure. The LT2 Aguas Calientes dacite was erupted on the south-eastern flank during the early stages of the last glacial maximum (30-25 ka) and shows strong evidence of interaction with ice. Extensive postglacial andesite lavas (LT3 and LT4a) form much of the LT edifice and extend down the Estero Renegado valley (Fig. 1). The source of these lavas has been buried by more recent cones but is referred to, as Volcán Democrático.

Volcán Viejo (LT4b) is the oldest of the summit crater structures and is geochemically linked with the Pata de Perro satellite cone and lava (LT4c) on the eastern flank. Holocene ($^{14}$C-dated) tephra fall sequences observed on the flanks and in valleys to the east are also geochemically correlated with Viejo and four recognisable fall units are described (H1-4), stratigraphically below Hc where found together. The dacitic stratocone Volcán Chillán (LT5a and LT5b) was constructed on the south-western crater-rim of Volcán Viejo and produced blocky dacite flows on the southern and south-western flanks. LT5b lavas are geochemically correlated with the LT5c Shangri-La lava and dome in the saddle.

Historic eruptions constructed Volcán Nuevo (1906-1943) and Volcán Arrau (1973-1986) on the remnants of Volcán Democrático.

## GEOCHRONOLOGY

Conventional $^{14}$C dating of 10 charcoal samples was carried out by Beta Analytic (Florida) and two Accelerated Mass Spectroscopy (AMS) analyses were obtained from the Oxford University Radiocarbon Accelerator Unit. The radiocarbon data are summarised in table 1. $^{40}$Ar/$^{39}$Ar analysis was carried out at the Scottish Universities Research Reactor Centre at East Kilbride, Scotland. The methodology is described in detail in Singer and Pringle (1996) and is summarised here. The samples were irradiated with monitor samples in the Oregon State University Triga reactor (neutron source) for 1 hour. This converted a significant proportion of the $^{40}$K present in the rock into $^{40}$Ar. These samples were then step heated under vacuum and the gases given off during each heating increment passed via chemical scrubbers into an ultra-sensitive rare gas mass-spectrometer. $^{36}$Ar, $^{37}$Ar, $^{39}$Ar and $^{40}$Ar were measured to provide data on initial gas content and argon generated by processes other than the slow-neutron bombardment of $^{40}$K. System blanks were read before all analyses, and analyses of reference standards irradiated in the same vials as the samples carried out to determine the neutron flux experienced by each sample. Data from each heating increment are plotted as apparent age against quantity of gas

**TABLE 1. SUMMARY OF RADIOCARBON SAMPLES AND RESULTS.**

| $^{14}C$ BP age* | Locality No. | Sample description |
|---|---|---|
| 8,950 ± 70 | 65 | Peaty soils within tephra fall section |
| 9,300 ± 70 | | |
| 8,200 ± 70 | | |
| 5,330 ± 70 | 74 | Peaty soils within tephra fall section |
| 5,790 ± 70 | | |
| 5,720 ± 60 | 164 | Peaty soils below tephra section |
| 8,920 ± 60 | 155 | Charcoal-bearing pyroclastic flow deposit |
| 2,270 ± 70 | 1401-3 | Charcoal-bearing pyroclastic flow deposit |
| 3,460 ± 60 | 137 | Charcoal-bearing pyroclastic flow deposit |
| 37,500 ± 500 | 44 | Carbonised logs in Nev2 Pleistocene ignimbrite |

* BP: Abbreviation of Before Present. Radiocarbon ages are conventionally specified to the year 1950, defined as 'present'.

released. These plots can only be considered to give valid 'plateau' ages if they meet four rigorous criteria as follows:

**i-** age spectrum plateaux are defined by, at least, three contiguous steps all concordant in age at the 95% confidence level and comprising >50% of the $^{39}Ar$ released.

**ii-** a well defined isochron exists for the plateau points as defined by the F-variate statistic SUMS/(N-2) for the York2 regression used.

**iii-** the plateau and isochron ages are concordant at the 95% confidence level.

**iv-** the $^{40}Ar/^{39}Ar$ intercept on the isochron diagram does not differ from the atmospheric value of 295.5 at the 95% confidence level.

$^{40}Ar/^{39}Ar$ analysis results are given in table 2.

## GEOCHEMISTRY AND PETROLOGY

Geochemical and petrological criteria were used to check correlations, in some instances to help define some of the stratigraphic units and in assigning lavas and pyroclastics of uncertain origin to specific units. These correlation methods were particularly useful in cases where geological constraints such as contact relations or source vents were ambiguous or concealed by more recent activity.

140 whole-rock samples were analysed by XRF and 80 petrographic thin-sections were examined under the optical microscope. A set of representative analyses is shown in table 3.

Nevados de Chillán has produced magmas with whole rock compositions ranging from basaltic andesite to low-silica rhyolite (53-71% $SiO_2$ normalised anhydrous). The data plot in the medium- to high-K fields of Gill (1981) (Fig. 3) and form calc-alkaline trends (Fig. 4), typical of subduction-related magmatism in this part of the Andes (Ferguson *et al.*, 1992; Tormey *et al.*, 1995). The CB subcomplex has erupted magmas with a continuous range of $SiO_2$ content, predominantly basaltic andesite to high-Si andesite with very minor dacite. The LT subcomplex has erupted a bimodal sequence, predominantly high-Si dacite to low-Si rhyolite accompanied by subordinate basaltic andesite and low-Si andesite. Only minor amounts of magma in the compositional range 58-66% $SiO_2$ has been erupted the LT subcomplex with the exception of mixed lavas of the LT5b and LT5c units (especially clear in $SiO_2$ *versus* $TiO_2$ plots - Fig. 4b).

Mineral assemblages are anhydrous throughout the sequence. Olivine (with Cr-spinel inclusions), plagioclase and clinopyroxene occur in the basic magmas. The intermediate rocks contain plagioclase and clinopyroxene±orthopyroxene± titanomagnetite±rare olivine. The silicic rocks contain plagioclase, two pyroxenes, titanomagnetite, ilmenite and apatite. The basic to intermediate rocks are generally medium to coarse-grained and porphyritic with holocrystalline or intersertal groundmass, except for some of the older subglacial andesites which are fine-grained and phenocryst-poor. The dacites are typically fine-grained and crystal-poor with intersertal groundmass textures.

**TABLE 2. $^{40}Ar/^{39}Ar$ ANALYSES.**

| | | Age Spectra | | | | | Isochron analysis | | | | |
|---|---|---|---|---|---|---|---|---|---|---|---|
| Sample No. | K/Ca (Total) | age (ka ± 1σ) | Increments used (°C) | $^{39}Ar$ (%) | Spectrum age (ka ± 1σ) | MSWD | N* | SUMS / (N-2) | $^{40}Ar/^{36}Ar$ Intercept ± 1σ | Age (ka)± 1σ** | Unit |
| C-8 | 0.345 | 22.3 ± 6.1 | 500-1200 | 90.4 | 0.6 ± 4.5 | 4.81 | 9 of 10 | 5.22 | 296.6 ± 1.5 | **-2.1 ± 5.7** | CB3b |
| C-25 | 0.088 | -46.2 ± 22.8 | 500-1250 | 100.0 | 34 ± 42 | 5.92 | 7 of 7 | 11.61 | 294.5 ± 2.2 | **8.2 ± 3.6** | CB2a |
| C-9 | 0.940 | 19.0 ± 2.6 | 600-1150 | 86.5 | 14.9 ± 0.9 | 0.78 | 10 of 12 | 0.71 | 296.5 ± 1.3 | **14.2 ± 1.1** | CB2b |
| C-27 | 0.312 | 53.1 ± 5.1 | 600-1100 | 86.8 | 26.2 ± 2.5 | 0.73 | 7 of 11 | 0.74 | 296.8 ± 0.8 | **23.9 ± 2.7** | CB2a |
| C-59 | 1.611 | 26.2 ± 1.1 | 525-1350 | 100.0 | 25.4 ± 0.7 | 0.58 | 7 of 7 | 0.35 | 297.4 ± 1.4 | 25.0 ± 0.8 | |
| C-59 | 1.567 | 27.1 ± 0.9 | 600-1125 | 95.2 | 25.8 ± 1.0 | 2.72 | 4 of 6 | 3.48 | 297.0 ± 10.8 | 25.4 ± 1.8 | |
| | | | | | 25.5 ± 0.6 | | | | C-59 weighted mean: | **25.1 ± 0.7** | LT2 |
| 97-33 | 3.085 | 21.1 ± 1.8 | 675-1025 | 80.7 | 27.5 ± 1.3 | 0.40 | 6 of 11 | 0.28 | 298.9 ± 7.4 | **26.2 ± 3.0** | LT2 |
| C-53 | 1.532 | 29.1 ± 1.2 | 500-1400 | 100.0 | 29.4 ± 1.0 | 0.82 | 9 of 9 | 0.84 | 294.0 ± 2.4 | 30.0 ± 1.6 | |
| C-53 | 1.694 | 30.5 ± 12.1 | 600-1000 | 97.4 | 30.3 ± 0.8 | 0.82 | 4 of 7 | 1.22 | 295.5 ± 2.3 | 30.3 ± 1.5 | |
| | | | | | 29.9 ± 0.6 | | | | C-53 weighted mean: | **30.2 ± 1.1** | LT2 |
| C-50 | 0.225 | 34.1 ± 13.7 | 500-1250 | 100.0 | 35.7 ± 6.3 | 3.54 | 7 of 7 | 4.89 | 294.4 ± 1.5 | 39.1 ± 8.6 | |
| C-50 | 0.242 | 41.9 ± 8.8 | 500-1325 | 100.0 | 42.6 ± 9.2 | 7.07 | 7 of 7 | 12.86 | 293.9 ± 1.3 | 43.7 ± 10.8 | |
| | | | | | 37.9 ± 5.2 | | | | C-50 weighted mean: | **40.9 ± 6.7** | LT1a |
| C-114 | 1.097 | 66.0 ± 1.1 | 750-1250 | 96.3 | 67.7 ± 1.0 | 3.30 | 5 of 8 | 2.94 | 283.1 ± 11.5 | **68.1 ± 1.0** | Nev1b |
| C-90 | 0.614 | 93.3 ± 1.7 | 825-1100 | 53.8 | 82.9 ± 1.8 | 0.37 | 4 of 9 | 0.56 | 296.8 ± 3.2 | **81.5 ±4.0** | CB1 |
| 97-16 | 0.576 | 96.6 ± 2.7 | 675-1125 | 85.0 | 87.6 ± 2.4 | 0.47 | 6 of 9 | 0.30 | 300.0 ± 12.0 | **85.3 ± 5.8** | Nev1a |
| C-44 | 0.258 | 426 ± 208 | 500-1025 | 70.6 | 271 ± 95 | 0.48 | 14 of 16 | 1.63 | 294.9 ± 1.7 | **157 ± 45** | LP[1] |
| C-18 | 0.519 | 420.0 ± 7.9 | 500-900 | 89.9 | 427 ± 6 | 33.0 | 6 of 9 | 37.90 | 305.0 ± 19.4 | **423 ± 10.8** | ?[2] |
| 97-01 | 0.279 | 803.3 ± 18.0 | 700-1100 | 45.0 | 640 ± 14 | 5.30 | 6 of 11 | 4.30 | 295.0 ± 1.5 | **641 ± 20** | LP |
| C-156a | 0.429 | 571.4 ± 302 | 500-1300 | 100.0 | 800 ± 165 | 7.23 | 11 of 11 | 20.80 | 295.7 ± 12.1 | **883 ± 283** | LP[3] |
| 97-13 | 0.266 | 2,697 ± 14 | 875-1400 | 67.9 | 2500 ± 60 | 55.0 | 8 of 14 | 69.40 | 324.0 ± 14.0 | **1,820 ± 320** | CZ[4] |

* Number of increments used in regression.

** Isochron ages are preferred; weighted means are from pairs of analyses.

All samples are whole-rock cores.

Analytical methods and data reduction are summarized in Singer and Pringle (1996).

All ages calculated relative to 27.92 Ma for Taylor Creek Rhyolite sanidine 85G0033.

1, 3, 4: Low-precision results from subglacial lavas, generally caused by large 'trapped-gas' components - included primarily for completeness.

2: Age from unit of uncertain provenance.

4: CZ = Cola de Zorro Formation.

**TABLE 3. SELECTED REPRESENTATIVE GEOCHEMICAL ANALYSES OF NEVADOS DE CHILLAN ROCKS.**

| Sample No. | C156a | C4 | C88 | C7 | C28 | C165D | C70 | C154a | C24 | C22 | C53 |
|---|---|---|---|---|---|---|---|---|---|---|---|
| Unit Name | LP | Nev1b | CB1 | CB2a | CB2b | CB3a | CB3b | CB3b | CB4 | LT1a | LT2 |
| $SiO_2$ | 60.6 | 67.9 | 58.6 | 57.9 | 65.6 | 66.0 | 56.4 | 56.0 | 56.7 | 53.0 | 69.3 |
| $TiO_2$ | 1.68 | 0.77 | 1.24 | 1.07 | 1.05 | 0.95 | 1.20 | 1.14 | 1.11 | 0.98 | 0.72 |
| $Al_2O_3$ | 15.4 | 15.3 | 16.9 | 17.2 | 15.3 | 15.3 | 19.3 | 17.8 | 17.6 | 18.3 | 15.0 |
| FeO | 7.29 | 3.86 | 7.02 | 6.99 | 5.07 | 4.91 | 6.82 | 7.42 | 7.43 | 7.89 | 3.35 |
| MnO | 0.13 | 0.11 | 0.13 | 0.12 | 0.11 | 0.10 | 0.11 | 0.13 | 0.13 | 0.14 | 0.10 |
| MgO | 2.34 | 0.94 | 3.28 | 3.89 | 1.43 | 1.41 | 2.65 | 4.47 | 4.12 | 6.11 | 0.77 |
| CaO | 5.26 | 2.74 | 6.51 | 7.01 | 3.64 | 3.61 | 8.00 | 7.95 | 7.59 | 8.96 | 2.36 |
| $Na_2O$ | 4.69 | 5.61 | 4.47 | 4.24 | 5.29 | 4.81 | 4.02 | 3.66 | 4.12 | 3.45 | 5.64 |
| $K_2O$ | 1.96 | 2.52 | 1.44 | 1.34 | 2.26 | 2.66 | 1.13 | 1.16 | 0.98 | 0.98 | 2.56 |
| $P_2O_5$ | 0.64 | 0.17 | 0.38 | 0.23 | 0.26 | 0.25 | 0.29 | 0.29 | 0.24 | 0.20 | 0.15 |
| Rb | 59 | 74 | 40 | 34 | 66 | 87 | 31 | 29 | 23 | 14 | 73 |
| Sr | 358 | 267 | 440 | 456 | 295 | 282 | 497 | 463 | 489 | 925 | 229 |
| Y | 28 | 33 | 24 | 20 | 30 | 26 | 19 | 17 | 17 | 14 | 34 |
| Zr | 235 | 289 | 172 | 159 | 247 | 287 | 138 | 121 | 129 | 118 | 268 |

| Sample No. | C17 | C52 | C146c | C99 | C1 | C14 | C5 | C190 | C68 | C158k | C139b |
|---|---|---|---|---|---|---|---|---|---|---|---|
| Unit Name | LT3 | LT4a | LT4b | LT4c | LT5a | LT5b | LT5b | LT6-7 | H2 | H(NE) | H4 |
| $SiO_2$ | 56.5 | 69.4 | 69.4 | 69.6 | 68.9 | 63.8 | 66.7 | 67.6 | 69.9 | 61.5 | 53.5 |
| $TiO_2$ | 1.14 | 0.68 | 0.71 | 0.74 | 0.66 | 0.86 | 0.80 | 0.88 | 0.63 | 1.11 | 1.32 |
| $Al_2O3$ | 17.5 | 14.5 | 14.6 | 14.4 | 14.8 | 15.6 | 15.0 | 15.0 | 14.6 | 17.5 | 21.4 |
| FeO | 7.48 | 3.85 | 3.85 | 3.86 | 3.84 | 5.19 | 4.49 | 4.40 | 3.69 | 6.10 | 8.47 |
| MnO | 0.13 | 0.09 | 0.09 | 0.09 | 0.09 | 0.10 | 0.09 | 0.09 | 0.09 | 0.13 | 0.13 |
| MgO | 4.27 | 0.68 | 0.67 | 0.74 | 0.87 | 2.55 | 1.67 | 1.05 | 0.60 | 2.11 | 3.70 |
| CaO | 7.62 | 2.18 | 2.29 | 2.29 | 2.48 | 4.80 | 3.58 | 2.95 | 2.09 | 4.56 | 6.97 |
| $Na_2O$ | 4.08 | 5.23 | 5.05 | 5.11 | 5.15 | 4.52 | 4.73 | 4.98 | 5.21 | 4.77 | 3.40 |
| $K_2O$ | 1.04 | 3.25 | 3.23 | 3.09 | 3.08 | 2.41 | 2.76 | 2.84 | 3.10 | 1.84 | 0.82 |
| $P_2O_5$ | 0.24 | 0.13 | 0.14 | 0.15 | 0.13 | 0.17 | 0.16 | 0.22 | 0.11 | 0.38 | 0.31 |
| Rb | 25 | 100 | 107 | 100 | 99 | 75 | 91 | 92 | 98 | 55 | 21 |
| Sr | 489 | 189 | 194 | 209 | 217 | 320 | 277 | 244 | 180 | 346 | 430 |
| Y | 18 | 36 | 30 | 34 | 33 | 26 | 30 | 27 | 30 | 28 | 21 |
| Zr | 133 | 334 | 330 | 331 | 300 | 258 | 301 | 311 | 332 | 237 | 155 |

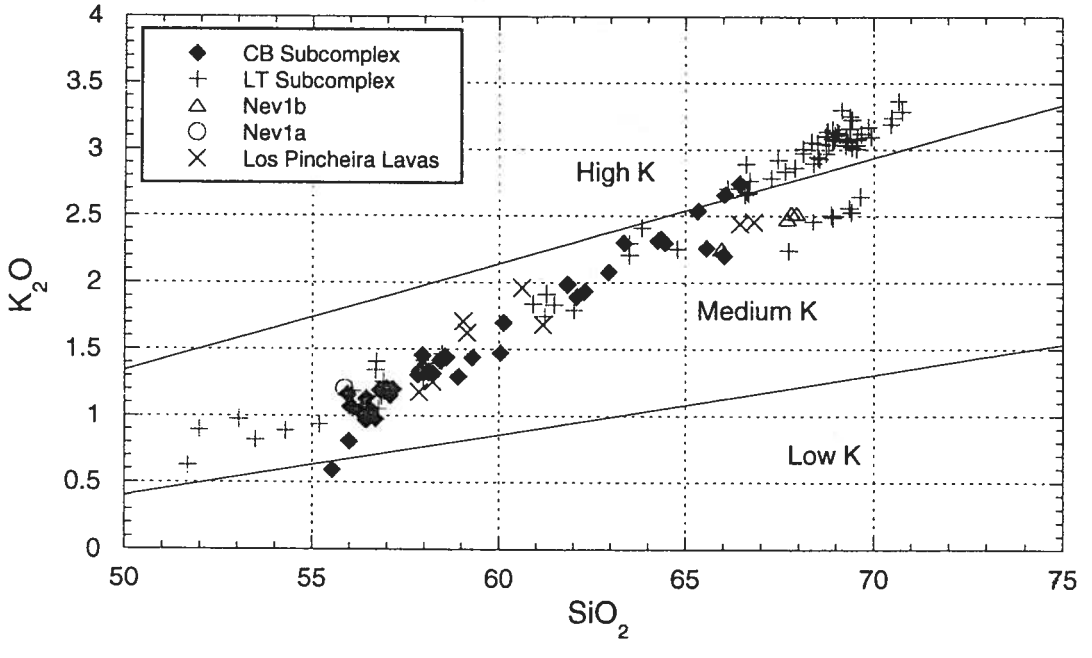


FIG. 3. $K_2O$-$SiO_2$ analyses, with high-, medium- and low-K fields after Gill (1981).

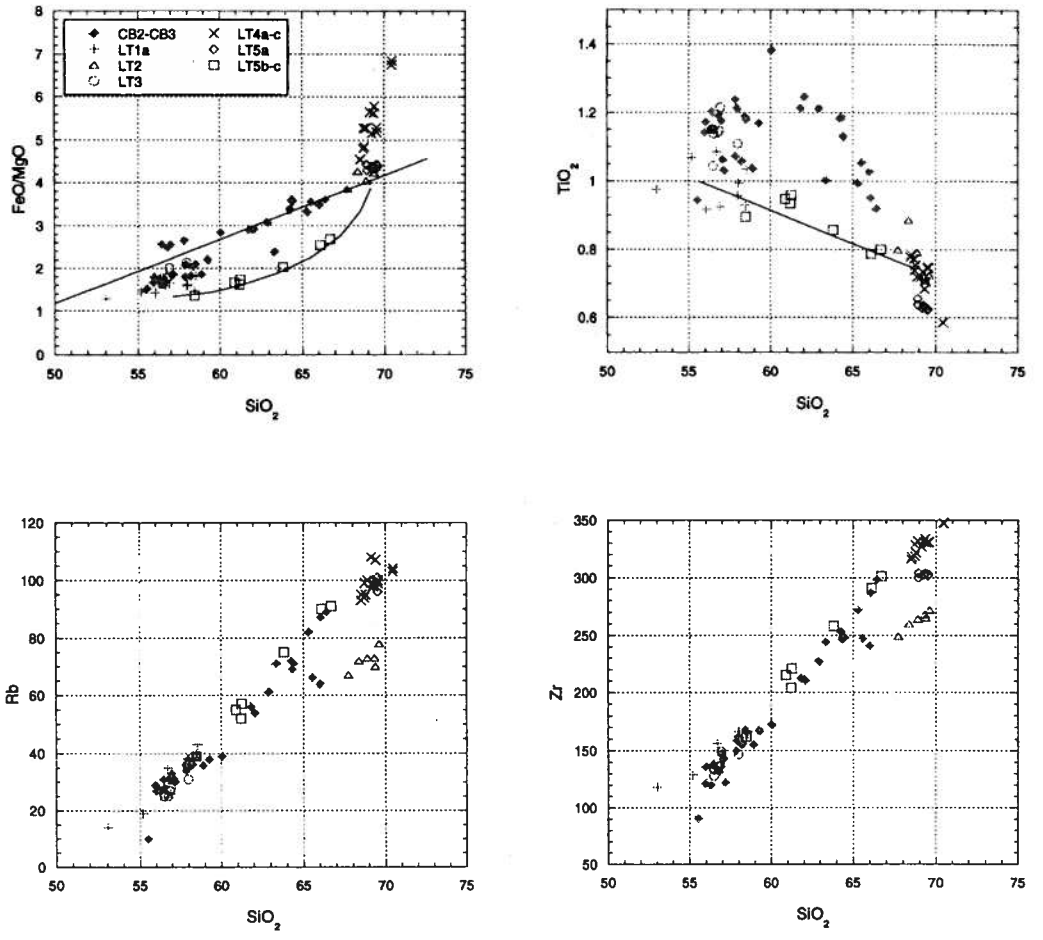


FIG. 4. Elemental variation diagrams (*versus* $SiO_2$); **a-** FeO*/Mgo. Tholeiitic/calcalkaline division after Miyashiro (1974). LT5a and LTSb samples form a hyperbolic mixing trend (curved line) distinct from all other units. [FeO is total Fe recalculated as FeO]; **b-** $TiO_2$. The LTSa-b mixing trend (line) is again clear; **c-** Rb. LT2 (open triangles) form a group distinct from the other LT units; **d-** Zr. The high-Zr LT4a-c dacites are quite distinct from LTSa samples. LTSb-c analyses form a strong trend toward the LT4a-c dacites, suggesting a possible evolutionary affinity.

Three correlation methods were used, often in combination, as illustrated below:

**1-** some groups of samples form distinctive trends on $SiO_2$ variation diagrams.

**2-** some groups of silicic samples have distinctive incompatible element abundances and ratios.

**3-** petrographic features allowed some samples to be correlated, especially intermediate rocks.

Rocks which display mixing trends between basaltic andesite and high-Si dacite are clearly distinguished on the FeO*/MgO and $TiO_2$ against $SiO_2$ plots (Figs. 4a, b). Most samples which fall on these trends also show petrographic evidence for magma mixing in the form of quench-textured mafic inclusions and/or disequilibrium mineral assemblages. In the latter case, forsteritic olivine (up to $Fo_{84}$) and sodic plagioclase ($An_{30-40}$) coexist, with plagioclase commonly showing resorption and reverse zonation. The samples with mixing trends are assigned to two stratigraphic units, the LT5b and LT5c units, which may ultimately have been sourced from the same magma chamber.

The LT high-Si dacites are distinguished from each other on the basis of their Rb and Zr contents. The older LT2 rocks have significantly lower Rb and Zr contents than the younger LT rhyodacites (Figs. 4c, d). The LT4 rocks are distinguished from the LT5a rocks by higher Zr at similar Rb. The mixed lavas of the LT5b and LT5c units also form a trend towards higher Zr, similar to the LT4 rocks.

Petrography was used to distinguish between several of the intermediate-composition units. In general, the subglacial Los Pincheira andesites are very crystal poor, whereas younger andesites tend to be coarse-grained and highly porphyritic. There are distinct differences in mineral assemblages at a similar $SiO_2$ content among some of the younger andesites. For example, titanomagnetite is very rare or absent in most samples with less than about 58% $SiO_2$, except for the LT1a unit. Orthopyroxene is rare or absent except in the LT1a and CB2a samples where it is abundant.

Correlation of proximal and distal pyroclastic deposits from the Viejo volcano was generally not definitive as there are no consistent differences between the horizons. However, some of the Viejo pyroclastics have an unusual high-Al, low-Ca geochemical signature, believed to be derived by incorporation of hydrothermally altered wallrock. This signature permitted distinction of some Viejo-derived basic to intermediate scoria deposits from CB scoria deposits.

## BASEMENT GEOLOGY

The basement geology of the area around Nevados de Chillán has been studied previously by other workers, including Gajardo (1981), and Muñoz and Niemeyer (1984). The Cretaceous and Tertiary volcanic rocks, sediments and granitic intrusive rocks of the area were not studied during this project, but form the glacially-eroded topography within which the Nevados de Chillán volcanic complex has developed.

The oldest rocks exposed in the area surrounding Nevados de Chillán are sediments of the Formación Cura-Mallín, consisting of conglomerates, breccias, sandstones, clays and tuffs with intercalations of limestone and andesitic-dacitic lavas. The age of the Formación Cura-Mallín has been given as Cretaceous by Gajardo (1981), and Eocene-Oligocene by Muñoz and Niemeyer (1984). Felsic plutonic rocks of the Santa Gertrudis batholith crop out extensively to the north and north-west of Nevados de Chillán. According to Muñoz and Niemeyer (1984), this batholith ranges in composition from granite to diorite and has yielded several radiometric ages of Lower Miocene age (15-17 Ma).

The Formación Cura-Mallín and the plutonic rocks are unconformably overlain by pyroclastics and lavas of predominantly andesitic composition assigned by the reconnaissance surveys of Gajardo (1981) and Muñoz and Niemeyer (1984) to the Formación Cola de Zorro. The formation is Pliocene to Upper Pleistocene in age and two K-Ar ages have been previously reported from within the vicinity of Nevados de Chillán: 0.49±0.26 Ma and 1.47±0.84 Ma (Gajardo, 1981). A $^{40}Ar/^{39}Ar$ age of 1.8±0.3 Ma was obtained during this work from an eroded subglacial hyaloclastite and pillow-breccia complex exposed high on the interfluve immediately to the south of the Río Renegado valley. The Los Pincheira group of valley-side bench lavas at Nevados de Chillán has a $^{40}Ar/^{39}Ar$ age of 640±20 ka (Table 2). The radial distribution of the Los Pincheira flows around Nevados de Chillán volcano clearly associates these lavas with the early development of the complex itself. The K-Ar age of 0.49±0.26 Ma reported from the Río Chillán valley by Gajardo (1981) came from a lava which is here assigned to the Los Pincheira group. A $^{40}Ar/^{39}Ar$ age of 423±10.8 ka (Table 2) was also obtained from an andesite lava on the north-eastern flanks. When more is known about the Formación Cola de Zorro, it is likely to be subdivided and some of the younger volcanic rocks assigned to specific long-lived volcanic centres. There are good geological and geographical grounds for including the Los Pincheira lavas as part of the Nevados de Chillán complex.

## GEOLOGY OF NEVADOS DE CHILLAN VOLCANO

### EARLY UNITS

#### LOS PINCHEIRA LAVAS

The Los Pincheira lavas are relatively thick, flat-topped flows forming valley-side benches bounded by steep cliffs. The unit has an estimated remaining volume of 10 km$^3$. As they have been heavily eroded, the original volume is likely to have been at least double than that estimated to remain. These andesitic lavas are very fine-grained, aphyric and often flinty or glassy. They are 100-200 m thick and exposed sections are characterised by a 50-100 m thick basal colonnade of well-developed columnar jointing, topped by an entablature of chaotic, hackly and irregular-columnar jointed material of a similar thickness (Fig. 5). The great thicknesses of the flows are interpreted as being due to subglacial ponding as the forward progress of the lavas was impeded by the need to melt glacial ice (cf. Lescinsky and Sisson, 1998). Meltwater formed during this emplacement would cause the development of fine-scale penetrative jointing of the entablature and the chilling of the groundmass. A $^{40}Ar/^{39}Ar$ age of 640±20 ka (Table 2) from locality 97-1 (Fig. 1) places eruption during isotope stage 16 of the global $\delta^{18}O$ record, a period of global ice accumulation, supporting the subglacial interpretation. In the Andean cordillera at this time, major regional ice sheets would have extended across the entire area (C.M. Clapperton, oral communication, 1996). Although major moraines have not been mapped in down-valley areas, the extensive drape of Pleistocene ignimbrites (See Nev2, below) may obscure most such features.

Gajardo (1981) obtained a low-precision K-Ar age of 490±260 ka from a lava in the Río Chillán valley which is here included in the Los Pincheira lavas. Another low-precision $^{40}Ar/^{39}Ar$ age of 883±283 ka from a thick bench-lava in upper Río Chillán valley was obtained during this work. The low precision was due to a large trapped-gas content swamping any radiogenic component. The low-precision K-Ar and $^{40}Ar/^{39}Ar$ ages are concordant with the high-precision 640 ka $^{40}Ar/^{39}Ar$ age to within errors. A $^{40}Ar/^{39}Ar$ age of 423±10.8 ka was obtained from an andesitic lava flow exposed on the north-eastern flanks of Cerro Blanco, but it is unclear what relation it bears to the Los Pincheira group. A much more extensive programme of sampling and $^{40}Ar/^{39}Ar$ analysis would be required to clarify the nature of early volcanism at Nevados de Chillán.

#### NEV1a ANDESITE

The Nev1a andesite (Fig. 1) forms a large (~1 km$^3$) eroded block on the south-western flanks of the volcano, truncated by vertical 50-100 m high cliffs. It is coarsely devitrified, with large-scale jointing

FIG. 5. Los Pincheira andesite in the Estero Renegado valley (locality C44), illustrating the sharp internal break between colonnade and entablature [cliff height ~ 125 m].

indicative of subaerial emplacement and slow cooling. $^{40}Ar/^{39}Ar$ geochronology yielded an age of 85.3±5.8 ka, prior to the start of isotope stage 4 of the $\delta^{18}O$ global climate record.

### NEV1b DACITE

Remnants of the Nev1b lava flow are exposed around the perimeter of the Shangri-La valley (Fig. 1), largely composed of columnar-jointed glassy lava. Remaining volume is estimated at 0.1-0.3 $km^3$. It is a crystal-poor dacite, with assemblages of plagioclase, clinopyroxene, orthopyroxene, titanomagnetite and ilmenite, similar to the other high-Si dacites but with slightly lower $SiO_2$ (66-68%). Basal exposures show 50 cm of coarse hyaloclastite breccia overlying 50-100 cm of glacial till. A 2-3 m thick basal colonnade of 0.5-1 m scale columns is topped by a complex set of curvilinear 10-25 cm scale columns, indicating highly distorted isotherms in the cooling lava flow (Fig. 6). The rapid and penetrative chilling implied by the scale of columnar-jointing indicates a voluminous source of cooling water. The exposures are the valley-marginal remnants of a single flow, the central part of which has been entirely removed by erosion. $^{40}Ar/^{39}Ar$ analysis yielded an age of 68.0±1.0 ka which places the eruption in isotope stage 4 of the marine $\delta^{18}O$ record, a period of increased global ice volume, consistent with the subglacial interpretation. Although stage 4 is thought to have been relatively weak on land, the field evidence indicates that at the 1,500 m altitude of this unit, glacial ice was present in this area.

These two lavas (Nev1a and 1b) are grouped together as their relationship to the Cerro Blanco and Las Termas subcomplexes is not established.

### NEV2 PLEISTOCENE IGNIMBRITES

There are two important areas of Pleistocene ignimbrite cover around Nevados de Chillán volcano though the distribution was not mapped in detail during this work. Excellent exposures of a carbon-bearing lithic-rich scoria and ash flow are preserved on top of the LP lava flows in the lower Estero Renegado valley, and further from the volcano to the west. Pumice flow deposits were also observed around 5 km to the north of the mapped area at San Fabián (Fig. 7) containing carbonised logs. An AMS radiocarbon age of 37,500±500 BP was obtained from material collected at locality 44, but no age could be determined for samples from San Fabián ($^{14}C$ age >40 ka). A large ignimbrite has also been identified in the Pleistocene fluvio-glacial deposits of the Central Valley of Chile, directly to the west of Nevados de Chillán. The deposits at locality 178 (Fig. 8) are non-welded pumiceous pyroclastic flow deposits with horizons of abundant charcoal. The Pleistocene ignimbrites may be linked to the putative caldera-collapse events associated with the cliffs cutting the LT1a and CB1 units (see below).

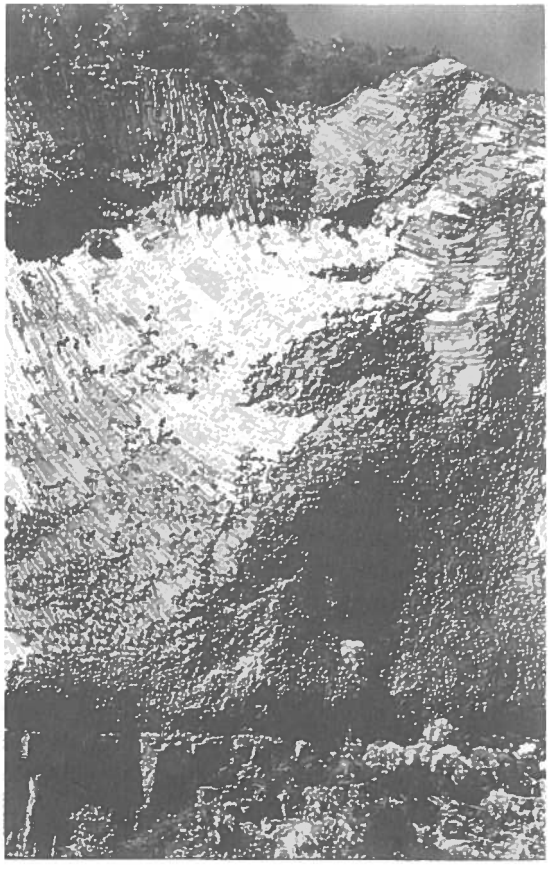

FIG. 6. Nev1b dacite at the southern side of the Shangri-La valley displaying curvilinear fine-columnar jointed entablature above a 3-4 m thick colonnade of 1 m scale columns [height of exposure ~ 25 m].

FIG. 7. Nev2 Pleistocene ignimbrite near San Fabián (*ca.* 10 km northwest of the volcano, off the top of the map figure). 1 m scale shown on metal tape measure.

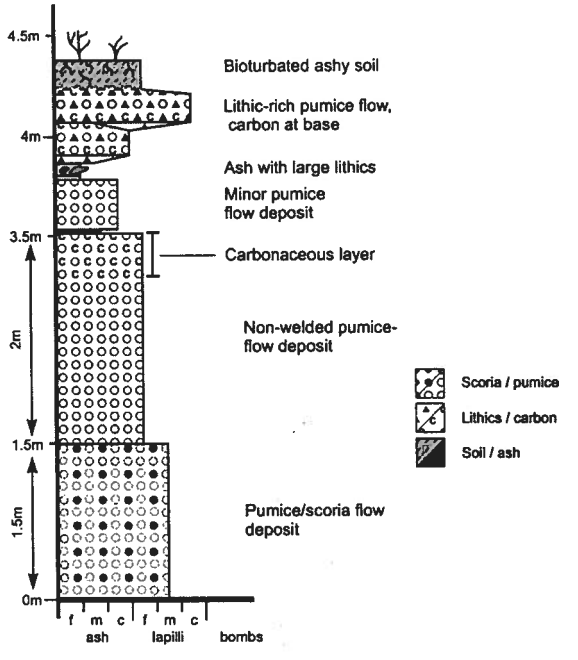


FIG. 8. Simplified log of the Nev2 pyroclastic flow section at locality 178.

## THE CERRO BLANCO SUBCOMPLEX

### CB1 LANALHUE UNIT

These lavas are exposed to the northwest and northeast of the Cerro Blanco subcomplex and are cut by 75-100 m high, arcuate, inward-facing cliffs (Fig. 9). The sequence comprises moderate thickness (2-3 m) individual andesite lava flows. They are crystal-poor andesites (58.1-62.3% $SiO_2$) with olivine, plagioclase and rare clinopyroxene. Subglacial hyaloclastic horizons and scoria layers also occur within the section. The lavas drape a strongly glaciated terrain of basement volcanic rocks and dip away from Cerro Blanco. A $^{40}Ar/^{39}Ar$ age of 81.5±4.0 ka has been obtained from near the base

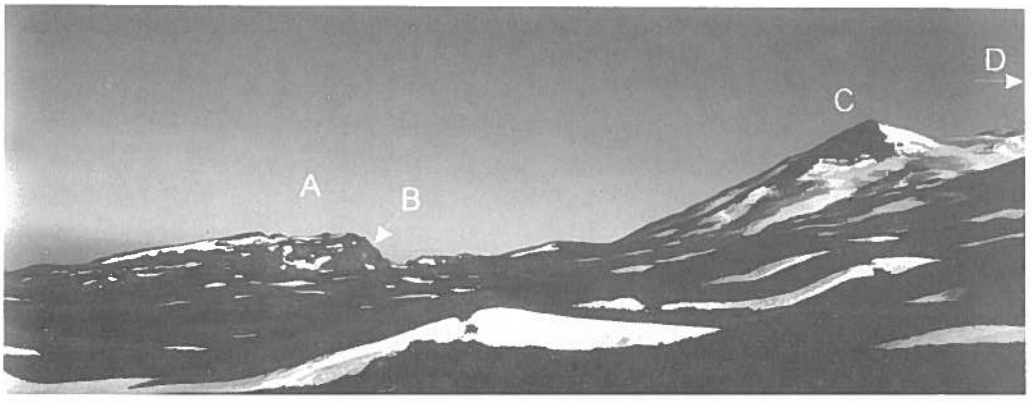


FIG. 9. View of the westward-dipping CB1 lavas (A) from the south-southeast, cut by the probable caldera cliffs (B) facing towards the somma block of the Colcura Stratocone (C) and the Cerro Blanco summit (D).

of the lava sequence. The cliffs cutting these lavas could be interpreted as remnant sectors of caldera wall (Déruelle and Déruelle, 1974). Their relationship to similar cliffs to the south of the volcano is not known, as the two lava sequences are not correlated.

### CB2 COLCURA AND EASTERN UNITS

The CB2 units form the bulk of the Cerro Blanco subcomplex edifice. CB2a lavas are remnants of a probable post-caldera-collapse shield volcano, mainly exposed in the north-east. The CB2b Colcura lavas are remnants of a steep-sided andesitic stratocone constructed upon this shield, together with lavas, breccias and debris deposits which extend *ca.* 20 to 25 km from the volcano in the deep glacial valleys. The CB2b stratocone probably underwent sector collapse, leaving several remnant blocks. The western block has a steep scarp facing toward the younger active edifice (Fig. 9) and is interpreted as a somma wall of the original crater. A monomict debris-avalanche deposit on the eastern flank is covered by younger (CB3a) lavas and may relate to the sector collapse of the Colcura structure. A $^{40}Ar/^{39}Ar$ age of 23.9±2.7 ka was obtained from a lava on the eastern flanks (CB2a) and an age of 14.2±1.1 ka from a CB2b flow in the Río Chillán valley. These lavas are porphyritic basaltic andesite to dacite (55.5-66% $SiO_2$) with assemblages of plagioclase, clinopyroxene±orthopyroxene±titanomagnetite± minor olivine±ilmenite.

### CB3 POST SOMMA UNITS

The uppermost Cerro Blanco subcomplex is constructed upon the eroded remains of the Colcura stratocone. A cliff section on the south-eastern flank of the Cerro Blanco edifice (Fig. 10) shows the top of the CB2b Colcura lavas with a sharp unconformity with overlying, more recent deposits (CB3). The edifice consists of a complex of andesitic and low-silica-dacitic stratocones each formed from intercalated lavas and pyroclastic ejecta. At least, three overlapping centres are distinguished: Calfú located on the southern flank; Gato, on the NNE side, and Blanco, which forms the summit of the edifice (Fig. 1). In the saddle, the Pichicalfú and Los Baños cones are linked to the young Cerro Blanco subcomplex on the basis of geochemical affinities. The Blanco and Gato cones have been grouped as one unit CB3a on the basis that they consist of indistinguishable low silica dacite (65.3-66.4% $SiO_2$). The Calfú, Pichicalfú and Los Baños cones have been grouped together as CB3b as they form a geochemically-distinct group of porphyritic mafic andesites (56-58.5% $SiO_2$), termed the 'Calfú type'. Assemblages are similar to CB2. The relative ages of these cones are not known, however, Calfú-composition scoria fall deposits form an important component of the Holocene tephra stratigraphy (see below).

FIG. 10. The sharp unconformity between CB2b Colcura and CB3a Cerro Blanco deposits, exposed on the upper flank of the Cerro Blanco subcomplex.

### CB4 SANTA GERTRUDIS UNIT

The Santa Gertrudis cone is 500 m below the summit cones on the northern flank of the Cerro Blanco subcomplex. An andesite lava flow was erupted from the vent during 1861-1862 (M.E. Petit-Breuilh)[4] and effusion of the lava was accompanied by Strombolian explosions and lahars generated by melting of snow and ice. The scoria cone at the source vent post-dates the lava flow and was formed during 1864 and 1865. The composition of the lava falls in the same geochemical group as the Calfú cone lavas and ejecta.

## THE LAS TERMAS SUBCOMPLEX

### LT1A SOUTHERN ANDESITE UNIT

These are glaciated, subaerial, basaltic-andesite and andesite lavas exposed in steep arcuate cliffs which face toward the active centre, the flows dipping at low angle away from the centre (Fig. 11). The cliffs are 150-200 m high and consist of 20-30 individual porphyritic basaltic andesite and andesite (53-59.1% $SiO_2$) lava flows ranging from a few metres to over 10 m in thickness. Mineral assemblages are plagioclase, clinopyroxene±ortho-

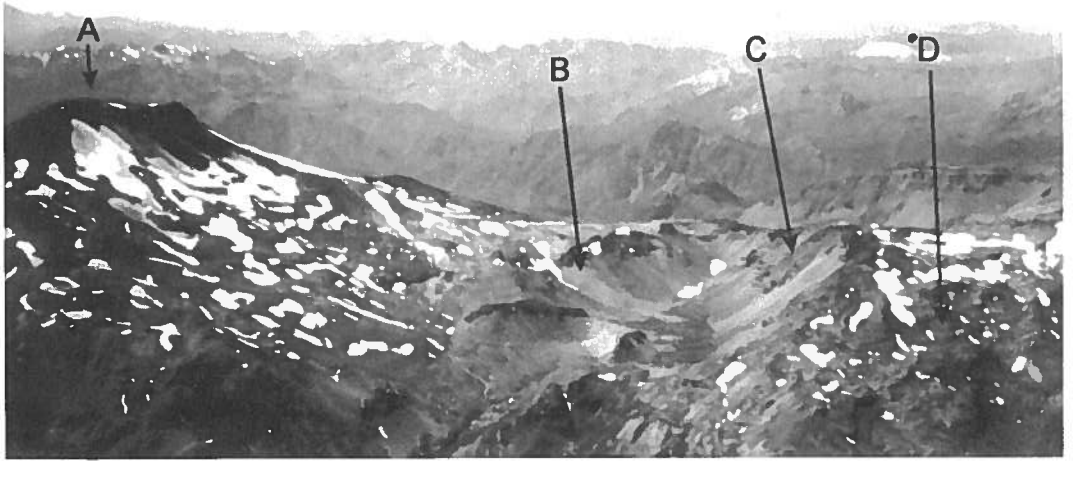


FIG. 11. An aerial view of the south-eastern Las Termas subcomplex from the south-west. Volcán Chillán (A) was constructed over the earlier material, of which the LT2 Aguas Calientes dacite (B) is exposed in the lower flanks. A possible sector of a caldera cliff (C) cuts the LTA Southern Andesites, dipping away (D) from the main complex.

[4] 1995. The volcanic history of Volcán Nevados de Chillán (Unpublished), *British Geological Survey*, p. 77. Keyworth, Nottingham, U.K.

pyroxene±titanomagnetite. Olivine is abundant in the more mafic samples, but rare in the andesites. A $^{40}Ar/^{39}Ar$ age of 40.9±6.7 ka has been determined for a lava from near the middle of the sequence. A minimally-glaciated scoriaceous horizon has been described from the top of the cliffs (C.M. Clapperton, oral communication, 1996), suggesting that the isotope-stage II glacial may have been relatively weak in this area. The cliffs must have been formed between the 40 ka age and the eruption of the Aguas Calientes lavas at 30 ka (see below). The arcuate, inward-facing cliffs could be the remnant sector of a caldera wall, but may be simply a consequence of glacial erosion.

#### LT1B LARQUI UNIT

This 150-200 m thick sequence of altered andesitic lavas, hyaloclastites, welded spatter and tephra fallout deposits forms a glacially-eroded triangular peak to the north-east of Nuevo cone and overlies highly altered basement lavas. The lava flows are typically 5-10 m thick, intercalated with 2-5 m thick welded fall-out and spatter deposits. The sequence dips at 20° to the north-north-east, suggesting that the unit is a remnant of an early stratovolcano. Its morphology and stratigraphic relationships indicate that it is probably equivalent in age to the southern andesites and may form part of an early large southern subcomplex, but no age data were available to confirm this.

#### LT2 AGUAS CALIENTES DACITE

This lava is exposed on the southern flanks of Volcán Chillán (Fig. 11). Upper flank exposures of the lava are composed of crystalline, devitrified material, with intensely frost-shattered platey jointing following the original flow banding. In the northern cliff face of Aguas Calientes valley, exposures of columnar jointed glassy dacite are found, some with associated hyaloclastite breccia. Complex radiating arrangements of columns (Fig. 12), indicative of penetrative water-cooling are exposed in a number of mounds on the lower slopes of the valley side. In general, the lower outcrops of the lava show a sequence from devitrified flow core to glassy columnar jointed exterior, in some cases with a carapace of hyaloclastite breccia intact. This is a similar sequence of facies to those described from subglacial acid hyaloclastites in Iceland (Furnes *et al.*, 1980). The field evidence suggests that the lava flowed subaerially on the upper flanks until it reached the cliffs and encountered the ice-filled valley. The flow may have then progressed onto the valley floor by melting a cavity at the edge of and underneath the ice body, developing the spectacular jointing due to chilling by meltwater. The radial-columnar-jointed mounds of glassy lava would have formed where lobes intruded the ice, and thus, were cooled by water on all sides. $^{40}Ar/^{39}Ar$ ages of 25.5±0.6 ka and 30.0±1.4 ka have been obtained from this unit, placing its eruption early during the last glacial

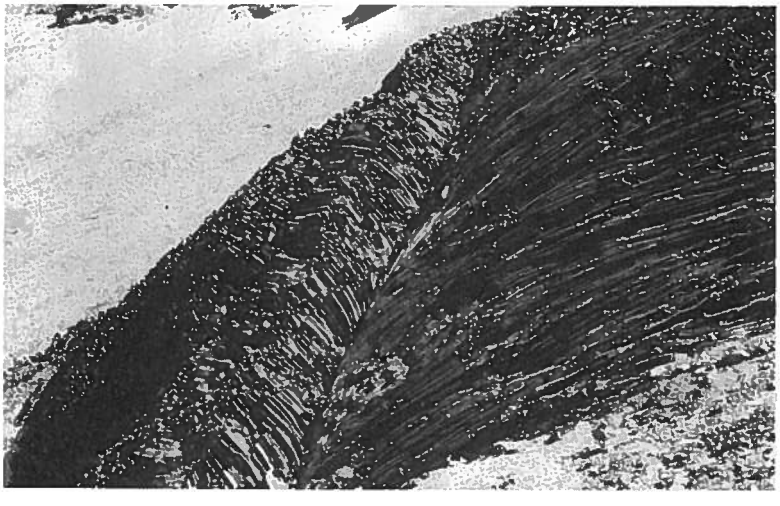

FIG. 12. 10-20 cm scale columnar jointed glassy dacite (LT2) exposed in the side of Aguas Calientes valley (close to locality 97-33).

(isotope stage 2). These are high-Si dacites (67.7-69.4% $SiO_2$), with mineral assemblages of plagioclase, clinopyroxene, orthopyroxene, titanomagnetite and ilmenite.

### LT3 DEMOCRATICO 1 LAVAS

This postglacial andesite unit comprises the eroded and largely buried remnants of a cone (Volcán Democrático) to the north of Viejo cone and extensive lavas to the east from the saddle and down the Renegado valley to the west. The Democrático structure was visible in pre-1973 aerial photographs, but is now almost entirely covered by the young LT6 and LT7 cones. In the saddle region, the lavas are heavily striated and smeared with moraine. Flow-fronts in the valleys are highly distinctive on aerial photos and are partly covered in extensive alluvium and lahar deposits. One lava can be traced over 35 km from Nevados de Chillán, the longest lava flow yet observed in the southern Andes (Naranjo *et al.*, 1994). These lavas are porphyritic mafic andesites (56.5-58% $SiO_2$), with phenocryst assemblages of plagioclase, clinopyroxene and minor olivine.

### LT4B VOLCAN VIEJO

The basal structure of the south-eastern Las Termas subcomplex (Fig. 1) is the Viejo stratocone composed of interstratified lavas and pyroclastic units including prominent densely welded andesite and dacite agglutinate layers. It is predominantly a dacitic pyroclastic edifice with two smaller craters, each around 250 m in diameter, nested within a 500 m. wide summit crater. Radiocarbon dating of geochemically-correlated Holocene tephra sequences indicate that Viejo is less than 9.3 ka old and continued its activity until, at least, 2,270 BP.

The lowest unit exposed in the core of Viejo consists of thick (up to 50 m), well bedded, grey, dacitic lapilli-tuffs with occasional block-rich beds. Individual clasts are angular, poorly- to non-vesicular glassy dacite. Bedding structures include planar-bedded units interpreted as primary fall out deposits, and large-scale cross-bedded units with foresets several metres in scale interpreted as subglacial hyaloclastites.

Subaerial pyroclastic deposits overlie the hyaloclastites. The distinctive geochemistry of these pyroclastics demonstrates that most of the Holocene tephras to the east of Viejo are also derived from this cone (see section on H1-H4 holocene tephra, below) and component-analysis indicates clear correlations between specific Viejo units and flank fall deposits. Three main facies were observed:

**i-** agglutinate beds produced by fountaining range from incipiently welded andesitic scoria and spatter to densely welded coarse lapilli-tuff with strongly flattened andesitic to dacitic fiamme.

**ii-** pumice fall deposits consisting of white, low density dacitic pumice block and lapilli breccias with minor proportions of lithics. Three deposits were observed within Viejo crater and a fourth deposit was erupted from a satellite vent immediately to the south of Viejo. The lowermost pumice deposit is linked by appearance and stratigraphic position with the H1 fall unit. The middle unit consists of a 100 m thick well-bedded fall deposit of pale yellow to white pumice (maximum dimension MP ~30 cm) with sparse fresh obsidian clasts and compositionally banded pumice. Beds vary from 30 cm to 1 m in thickness and number more than 100. Distinctive white pumices and obsidian chips link this with H2 tephra fall. The uppermost pumice deposit drapes the crater wall and is, therefore, younger than the Viejo summit-crater structure. The unit is (5 m thick, and is correlated with the sponge pumice deposit of the Holocene sequence (H3), as it is similarly dominated by 'spongy' pumices (see below).

**iii-** the third facies consists of two thick vulcanian deposits, a mixture of dense juvenile dacite blocks and accidental lithics. The most prominent examples occur above and below the youngest pumice deposit on the summit of Viejo cone (Fig. 12). The upper vulcanian deposit is correlated with the mafic scoriaceous tephra H4 of the Holocene tephra sequence to the east on the basis of stratigraphic position and geochemistry. The deposit (5 m thick) consists of 50-100 cm beds of coarse breccia, scoria and lithic lapilli. Dacitic breadcrust bombs are common. These deposits are associated with formation of the youngest Viejo crater.

### LT4A DEMOCRATICO 2 AND LT4C PATA DE PERRO LAVAS

These units are high-silica dacite lava flows on the south-western and south-eastern flanks of the Las Termas subcomplex and are grouped together on the basis of their similar geochemistry. The lavas are high-Si dacites to low-Si rhyolites (66.6-70.7% $SiO_2$), mostly crystal-poor, with assemblages of plagioclase, clinopyroxene, orthopyroxene, titanomagnetite and ilmenite.

The Democrático 2 lavas (LT4a) are found on the south-western flanks of the Las Termas edifice and are considered to have come from the same area as the LT3 Democrático 1 lavas.

The Pata de Perro lava flow (LT4c) was erupted on the south-eastern flank and extends to the headwaters of the Río Las Minas (Fig. 1). The upper part of the lava flow is overlain by the welded-pyroclastic Pata de Perro cone. The sources may form a complementary vent system, with explosive activity at Volcán Viejo and lava extrusion at the Democrático and Pata de Perro flank vents. The Pata de Perro lava flow is bracketed by the sequence of Holocene tephra fall deposits erupted from Volcán Viejo (H1-H4, see below).

### LT5A LOWER CHILLAN LAVAS

These blocky lavas outcrop on the south-west flanks of Volcán Chillán (Fig. 1) and represent early products of this cone, interstratified with reworked ash and pumice deposits. They are crystal-poor high-Si dacites (69-69.5% $SiO_2$), with assemblages of plagioclase, clinopyroxene, orthopyroxene, titanomagnetite and ilmenite.

### LT5B UPPER CHILLAN AND LT5C SHANGRI-LA LAVA

These two map units of blocky dacite have similar field appearances, occur in the same stratigraphic position and fall in a distinctive geochemical group (Fig. 4), but were erupted from geographically separate sources. The Shangri-La lava flow (LT5c) was erupted from a vent in the saddle region and flowed down the Shangri-La valley. The Upper Chillán lavas (LT5b) form the main structure of Volcán Chillán. The lavas are distinguished by the presence of abundant mafic inclusions and clots of mafic xenocrysts. The lavas have disequilibrium mineral assemblages of high-Mg olivine derived from mafic magma coexisting with plagioclase, pyroxene and Fe-Ti-oxides derived from dacitic magma. Mafic inclusions locally make up as much as 15% of the rock, although a few percent is more typical. The inclusions are predominantly ellipsoidal and range in size from less than 1 mm to *ca.* 50 cm diameter. Evidence that the inclusions were molten when incorporated into the dacite includes their typical rounded shapes, the presence of chilled and crenulate margins, the diktytaxitic textures and the occurrence of xenocrysts derived from the host dacite within the inclusions (cf. Bacon, 1986; Blundy and Sparks, 1992). Mixing calculations indicate that the silicic end-members in the LT5b and LT5c lavas permit derivation of these from the same magma body as the LT4 dacites (Fig. 4).

### LT6 VOLCAN NUEVO

This 180 m conical dacite lava dome complex (Fig. 2) and associated lava flow apron overlies the remnants of Volcán Democrático. Dome-building activity began in 1906 with sporadic activity extending to 1943, with minor explosive eruptions from the 100 m wide summit crater. The complex has steep (35-40°) flanks of coulée lavas and avalanche deposits.

### LT7 VOLCAN ARRAU

Arrau is a dacite lava cone constructed between Nuevo and Chillán Viejo volcanoes and on top of Volcán Democrático. It was erupted between 1973 (Déruelle, 1977) and 1986, reaching its maximum altitude in 1983 (Naranjo *et al.*, 1994). Its conic shape is a consequence of coulée lava flows as well as several hot avalanche deposits generated by pulses of dome growth and collapse that smoothed the flank surfaces. The lava cone has a steep (~35-40°) slope in its upper part and a 120 m wide summit crater.

The lavas of both Nuevo and Arrau volcanoes are glassy block-flows infiltrated by pumice and ash. They are medium-Si dacites (66.6-67.6% $SiO_2$) with mineral assemblages similar to the high-Si dacites, but they tend to be more crystal-rich.

## HOLOCENE TEPHRA DEPOSITS

### SATELLITE PYROCLASTIC CONES

Small pyroclastic cones occur on the outer flanks of Nevados de Chillán volcano and are mantled by the Holocene tephra sequence. Los Cuervos cone (8 km north-east of Volcán Nuevo), Las Lagunillas cone (5 km east of the saddle region) and the Parador cone (in the upper Shangri-La valley, 4 km to the south-west of the saddle) are oxidised andesitic scoria and spatter cones. Volcán Niblinto (north-west of the Cerro Blanco complex) is considered a separate centre, lying along the same NNW-SSE trend as the volcanic centres of Nevados de Chillán.

### TEPHRA FALL SEQUENCES

Holocene tephra fall deposits are primarily east and south of Nevados de Chillán, a distribution controlled by regional winds. Four main pumice fall deposits (H1-H4) topped by a sequence of vulcanian ashes were recognised. The authors' primary measured section is at locality 169 (Fig. 13). A reconnaissance study of the tephra fall deposits to the north-east indicated the presence of another sequence which cannot be directly matched with H1-H4, but which has geochemical features of high Al and Zr and low Ca and Sr which suggest that Volcán Viejo was the source. A measured section from locality 158 is shown in figure 14. A brief field investigation was carried out in Argentina, approximately 70 km east of the volcano, but no Nevados de Chillán tephra were found. Although detailed surveying was not carried out, the thicknesses and grain-sizes of the pumice fall deposits rapidly decrease with distance from the source (decreasing to 5 cm in thickness and ~15 mm maximum pumice dimension at around 10 km to the east of Volcán Viejo). The eruptions are interpreted as subplinian and vulcanian (Walker, 1973) on the basis of their limited dispersal, constituents and field appearance. Intercalated organic material was $^{14}C$ dated to constrain the ages of the fall units.

### SOUTH-EASTERN SEQUENCE

**Unit H1-Yellow Pumice Fall.** This normal graded lapilli deposit consists of broken, angular, yellow-white dacitic pumices and is commonly rich in lithics of angular hydrothermally-altered lava and weathered obsidians. Fall unit H1 is geochemically correlated with Volcán Viejo and considered equivalent to the lowest pumice fall deposit within the Viejo cone as it underlies the Holocene sequence and contains a similar range of clasts. The maximum non-proximal thickness found was 250 cm at locality 169. Downwind locality 155 shows a thickness fall to less than 5 cm.

**Unit H2-White Pumice Fall.** This deposit is characterised by white, tabular dacitic pumice lapilli, minor compositionally banded pumice near the top and a lithic-poor character with lithics being mostly juvenile fresh obsidian. This unit is geochemically correlated with the thick (100 m) middle pumice deposit exposed in Volcán Viejo. H2 is overlain by the Pata de Perro (LT4c) lava flow at locality 170.

**Unit H3 - Sponge Pumice Fall.** This lapilli deposit consists of white dacitic pumices with a spongy internal texture reflecting a high proportion a narrow size range (1-2 mm) of spherical vesicles. The deposit is generally well sorted with sparse lithics and minor juvenile obsidian fragments. Its thickness is ~12 cm in the proximal area, decreasing to 7 cm at locality 169. The pumice composition is characteristic of Volcán Viejo. The deposit is correlated with the youngest white dacitic pumice deposit which drapes the summit crater of the Viejo cone. H3 pumice overlies the Pata de Perro (LT4c) lava at locality 170.

**Unit H4 - Brown Pumice Fall.** This unit is a basaltic andesite scoria (~53% $SiO_2$) fall deposit with a substantial ashy component. Scorias are typically brown and platy or elongate (akin to thick ribbons). The scoria has the same composition as the youngest scoriaceous vulcanian deposit at the summit of Volcán Viejo, with which it is therefore correlated. Commonly this topmost surficial unit is reworked.

**Vulcanian Ashes.** Good exposures of these ashfall deposits are only found in lower-altitude exposures, where they have not been stripped off by erosion. Elsewhere, they contribute to the reworked ashy pumice debris that covers most exposed surfaces. Their source is inferred to be predominantly from the LT centres and they are likely to include ejecta from Viejo, Chillán, Nuevo and Arrau cones.

**Unit Hc - 'Calfú' Scoria.** A young andesitic scoria fall deposit occurs at the tops of several sections.

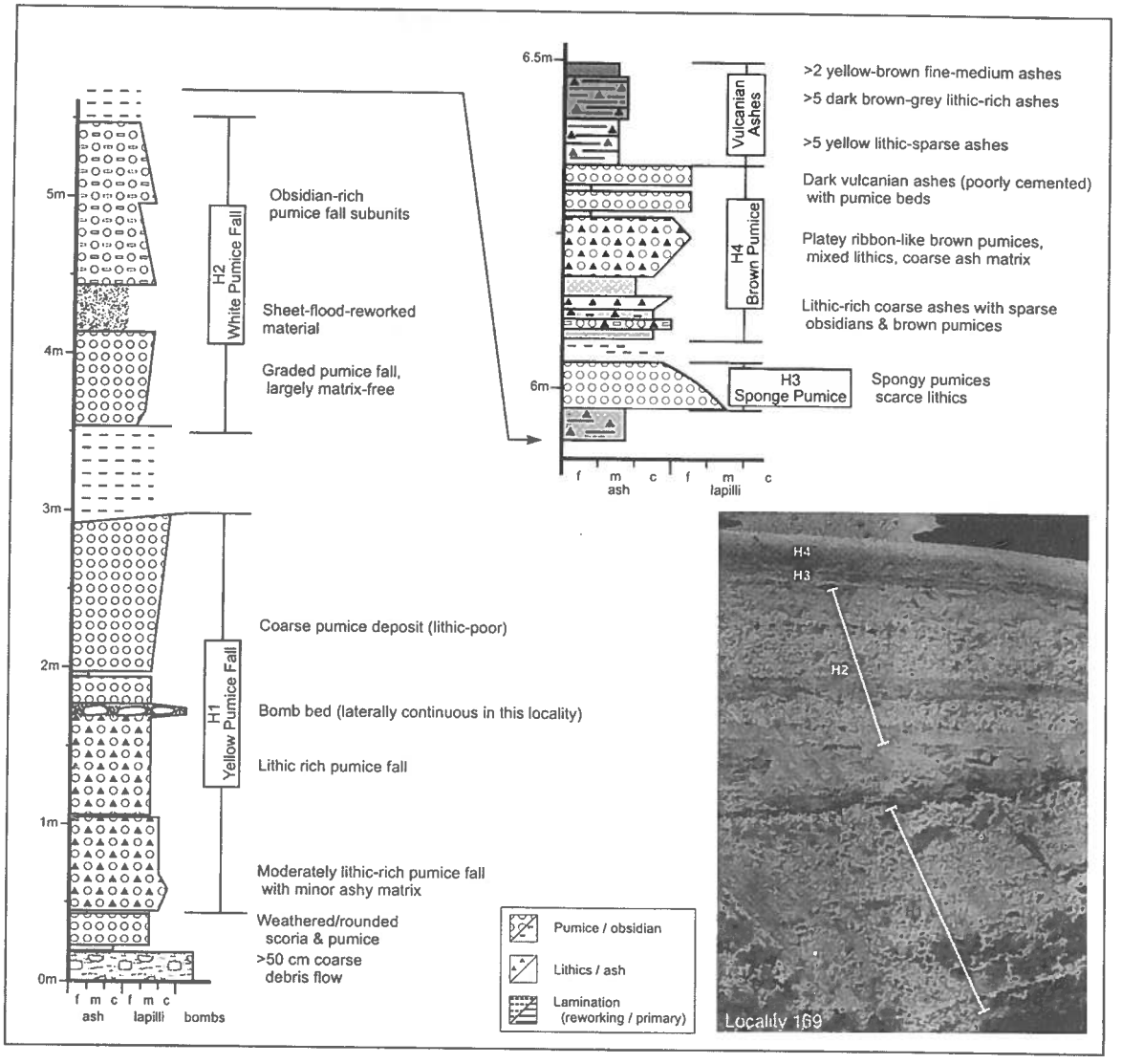


FIG. 13. H1-4 Holocene tephra fall and vulcanian ash sequence at locality 169 (reference section).

The deposit mantles the CB3b Los Baños cone in the saddle region and has characteristic 'Calfú' geochemistry. It is related either to the eruption of the CB3b Calfú cone itself or perhaps to the Santa Gertrudis vent (CB4).

## NORTH-EASTERN SEQUENCE

This tephra fall sequence (Fig. 14) has not been correlated with the sequence described above, as it appears sufficiently different in terms of physical composition. However, the pumices have the same geochemistry as H1-H3 with the distinctive high Zr characteristic of Viejo dacitic ejecta. Possible correlations of some of the fall subunits are included in figure 14.

## PYROCLASTIC FLOW DEPOSITS

Pyroclastic flow deposits of various ages and states of preservation were observed throughout the area. To the north and west of Nevados de Chillán, much of the area is mantled with highly weathered pyroclastic flow deposits. On Nevados de Chillán non-welded pyroclastic flow deposits are generally completely removed in proximal areas, and only

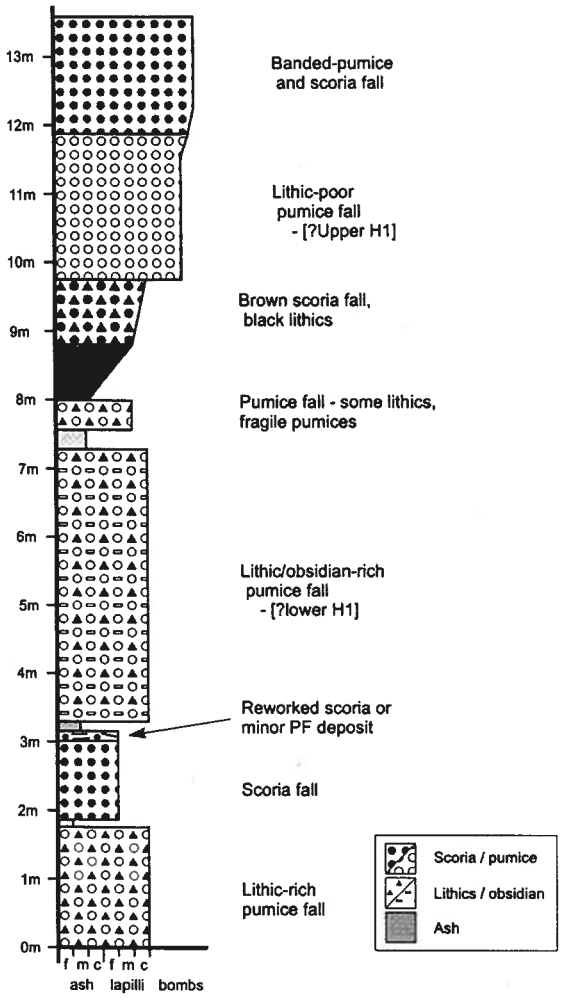


FIG. I4. Holocene tephra sequence at locality 158 [speculative compositional correlations with H1-4 sequence in brackets]. Note contrast of scale with figure 13.

locally preserved in the valleys or as drapes over the surrounding vegetated terrain. They are highly susceptible to weathering, so tend to develop into thick soils. The presence of charcoal and rounded scoria/pumice are often the only diagnostic features. Some thick, valley-ponded deposits remain fresh and preserve features such as scoria and lithic concentration zones, flow unit boundaries and gas-escape structures.

A scoriaceous surge deposit was found interstratified with the Holocene tephra fall sequence on the upper eastern flanks of the Las Termas subcomplex at locality 159 (Fig. 15). The deposit is fine grained, poorly sorted and well bedded (5-40 cm scale). Two fine-grained andesitic scoriaceous pyroclastic flow deposits are interstratified with the H2 and H3 pumice fall units in the Ñuble valley (Locality 155, Fig. 16a) and contain abundant charcoal giving a radiocarbon age of 8,920±60 BP (Table 1).

## AGE CONSTRAINTS ON HOLOCENE VOLCANISM

$^{14}C$ ages are summarised in table 1 and their stratigraphic positions in figures 16a-f. There are three groupings of Holocene ages: the first at around 9,000 BP at the base of the Holocene sequence (Fig. 16b); the second at 5,500 BP, bracketing the H1 and H2 deposits; and the third (looser) grouping at 2,000-3,500 BP obtained from proximal pyroclastic flow deposits. H1 and H2 must have been deposited within a very short time-span as the age below H1 at locality 164 (Fig. 16c) is 5,720±60 BP and the age above H2 at locality 74 (Fig. 16d) is 5,790±70 BP. To the west of Nevados de Chillán, within *ca.* 15 km of the volcano, localities 1401-3 and 137 (Figs. 16e-f) give ages of 2,270±70 and 3,460±60 BP for the most recent pyroclastic flows. The LT3 (Democrático 1) lavas are constrained to be older than 3,500 yr (Fig. 16f) and the Pata de Perro lava (LT4c) is younger than 5,500 BP as it overlies H2.

## MORAINES

Recent moraines high on the volcano are associated with the present-day seasonal mountain glaciers and contain locally reworked pyroclastic debris. In the high valleys (*e.g.*, Aguas Calientes), recent-glacial moraine lobes were noted, covered only by the Holocene tephra fall deposits. Younger small-scale moraines with no tephra cover may be due to late Holocene readvances (*e.g.*, Little Ice Age). Further afield, comparatively little unmodified glacial material is exposed. River-cut sections tend to show highly reworked glacio-fluvial gravels and cobble beds. Elsewhere, the surface is generally blanketed in altered pyroclastic flow deposits. These frequently include lithics derived from moraines, but generally obscure moraines which would quantify the large-scale Pleistocene ice cover around Nevados de Chillán.

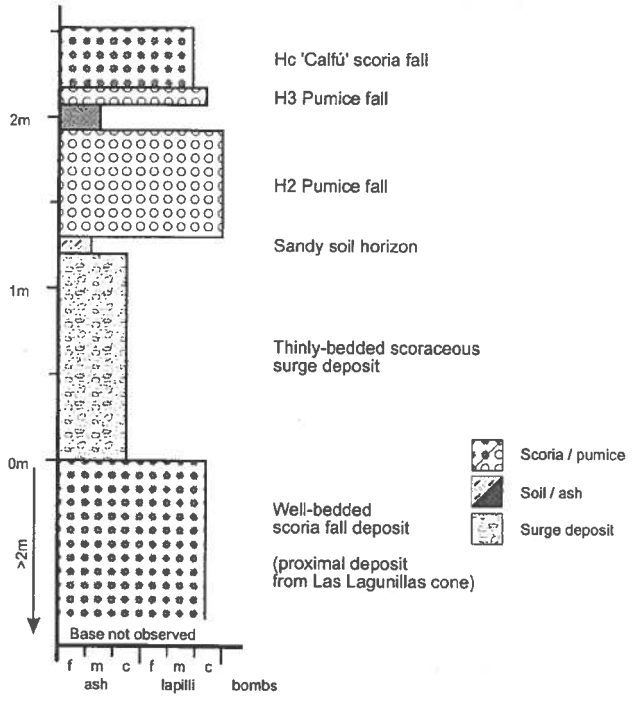


FIG. 15. Section at locality IS9 showing H2-3 and Hc sequence above proximal deposits from Las Lagunillas satellite cone.

## LAHARS AND ALLUVIUM

Remnants of lahar deposits occur in most river valleys. In the Estero Renegado valley, lahar deposits form large terraces through which the present streams and rivers have cut. A well exposed sequence of laharic deposits was observed (Fig. 17) in the upper Renegado valley. The lower unit is a coarse boulder deposit, 1.5 m thick, overlain by 40 cm of coarse sand (hyperconcentrated part of flow) in the usual twofold division of gravelly lahars. The lowest deposit contains poorly sorted boulders of Volcán Chillán lavas (LT5a) as well as older grey-weathered volcanic clasts. The upper sandy division has planar stratification implying an origin in the stream flood phase of deposition. This is better sorted and stratified than typical for a hyperconcentrated flow, and probably originates in the waning phase of the debris flow. The 'flood plain' of the small stream that now occupies this valley is littered with dead trees, most likely washed down in the last laharic flood event. Further, the trees growing above the 10 m terrace level are considerably more mature than those growing on the terrace surface. Using tree-rings at locality 135 (Fig. 17) to estimate the age of deposition of the terrace gave 300-400 years. The saplings growing on the lowest deposits suggest an age of, at most, a few tens of years for this more recent feature. Away from the stream course, trial-pits had been dug by quarriers, enabling observation of the deposits of the laharic flood plain. Two lithofacies were noted:

**1-** the lower unit is a laharic sheet-flood facies, representing a single depositional event. This was characterised by more massive, orange-oxidised beds, 10-40 cm thick. Crude internal stratification was noted in some parts of the deposit. The deposit was composed of coarse-medium sand and small pebbles, with mud drapes at the top of the unit.

**2-** the upper unit is a fluvial sheet wash facies, characterised by coarse, well-sorted and strongly laminated sand and pebbles (up to 10 cm), and well developed cross-beds.

## LANDSLIPS

In *ca.* 1990 a large volume of intensely hydrothermally-altered material failed on the slopes above the hot spring baths and hotels at Termas de Chillán. The debris avalanche produced, travelled 6-7 km down the valley, causing extensive damage to property. The present slope appears highly unstable, and is located directly above a newly-built hotel and a hot-spring complex.

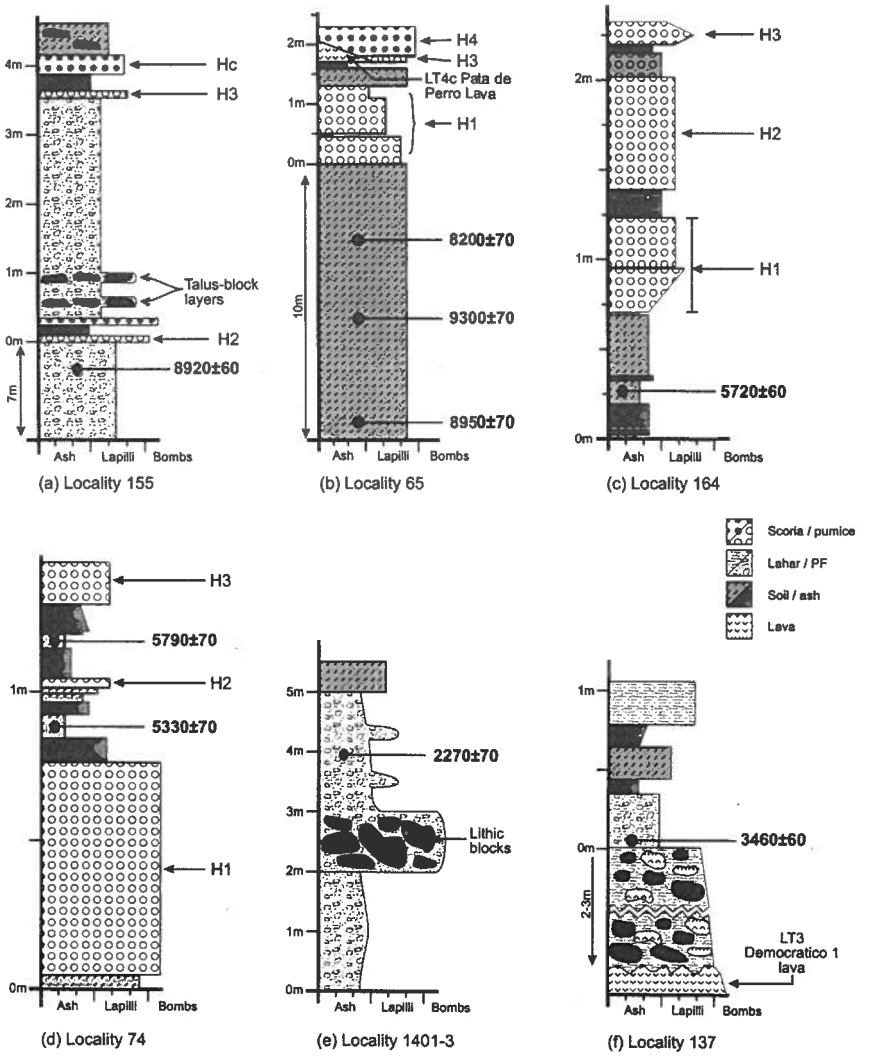


FIG. 16. Sections indicating stratigraphic positions of $^{14}C$-dated samples.Ages in years BP (Before Present).

FIG. 17. Lahar deposits forming a well-defined terrace in the upper Estero Renegado valley at locality 135.

## DISCUSSION

This study of the Nevados de Chillán complex has combined several techniques to elucidate some of the key features of the evolution of a large Andean volcano. Multi-disciplinary study, involving photogeology, geochemistry and petrology, and geochronology has yielded results beyond those possible purely from mapping. Geochemical and petrographic observations allow the identification of contemporaneous eruptions from separate vents such as Volcán Chillán and the Shangri-La dome and the distinction of otherwise similar glassy-block dacite flows.

A much more detailed geochronological and geological mapping study would be required to elucidate the early (>100 ka) activity of the volcanic centre. Comparison with study of the Tatara-San Pedro complex (Singer *et al.*, 1997) is instructive. Tatara-San Pedro has a fragmented record of older lavas extending to 930 ka, as major glaciations have eroded much of the material. The authors' data hint at a similarly extended, but partial record for Volcán Nevados de Chillán.

There remain several unresolved issues concerning the development of the complex in the post-100 ka period. It is, for example, unclear when the two currently active subcomplexes developed as independent centres. Some of the older lavas around the volcano cannot be assigned to either subcomplex. There are two sectors (4 major segments) of inward-facing cliffs, to the north-west, north-east and south-east. Lavas from the north-eastern cliff sections (CB1) are assigned to the early stages of the CB subcomplex, but overlap in age with the Nev1a and Nev1b lavas which are not assigned to either subcomplex. Lavas in the southern cliffs (LT1a) and on the eastern flanks (LT1b) are assigned to the early stages of the LT subcomplex. It is possible that the cliffs represent caldera walls as proposed by Déruelle and Déruelle (1974). The ages of lavas within the cliffs and lavas younger than the cliffs are consistent with an interpretation of caldera collapse related to the widespread Pleistocene ignimbrites (Nev2) erupted around 40 ka. Further studies will be required to test the caldera-formation hypothesis and to evaluate whether there were separate caldera-forming events associated with the early evolution of each subcomplex or a single major collapse over the entire volcanic complex.

Lava-ice interaction has played a key role in the geomorphological evolution of the volcano and the surrounding valleys. The thick lava benches along the valley sides show strong evidence of having been emplaced beneath thick valley glaciers or larger ice sheets (cf. Lescinsky and Sisson, 1998). The thickness of the flows (up to 200 m) compared to 25-50 m for similar andesite flows from the same volcano strongly suggests that the forward flow of the lavas was impeded, most probably by the need to melt a cavity into glacial ice. The internal jointing and chilled groundmass imply rapid cooling by a penetrative fluid. Similar field evidence of the interaction of lava and ice during eruptions was observed higher on the flanks of the volcano. Initially subaerial flows which encountered ice during downslope flow were abruptly cooled to produce thicker sections of spectacular columnar- and hackly-jointed structures.

High-precision $^{40}Ar/^{39}Ar$ analysis has enabled direct comparison between the field sequences of subaerial and ice-affected lavas and the global $\delta^{18}O$ oxygen record. Good agreement is seen between interpreted lava-ice interaction and global ice volume maxima, and between subaerial eruptions and interglacial periods, leading to the suggestion that subglacial volcanic rocks may be $^{40}Ar/^{39}Ar$-dated to constrain glacial histories.

Ice-chilled volcanism at Nevados de Chillán displays significant differences of scale and structure when compared to Icelandic subglacial basaltic volcanism (*e.g.*, Sigvaldason, 1968; Walker and Blake, 1966; Werner *et al.*, 1996). Within the hyaloclastite breccia there are large bodies (~10-50 m scale) of undisturbed, but intensely and pervasively fractured glassy lava. These show distinctive evidence of penetrative cooling by water (joint sets with secondary jointing networks indicative of sudden changes in thermal stress), but not the total disaggregation and hydroexplosive fragmentation invariably seen in Icelandic basalt hyaloclastite. A significant factor in the development of the lava-ice structures at Nevados de Chillán is the intermediate (andesite-dacite) composition of the lavas involved. The cooler eruption temperatures, higher viscosity

and slower eruption rates favour larger-scale structures and features given a similar cooling environment. Further, the geomorphology of the glacial environment (the slopes, peaks and valleys of the Andean Cordillera rather than relatively wide, flat expanses of Icelandic rift-zones) may explain some of the difference in morphologies of the products of lava-ice interaction such as thick, columnar lava flows rather than the development of table mountains or Tindar ridges (Jones, 1969). The ice-affected lavas have internal structures and forms more in common with subglacial lavas described from Antarctica (Smellie *et al.*, 1993; Smellie *et al.*, 1998) and Mount Rainier in the U.S.A. (Lescinsky and Sisson, 1998) than Icelandic table-mountains. In particular, valley-confined lavas from Northern Alexander Land, Antarctica (Smellie *et al.*, 1993) are similar in both thickness and internal structure to the Los Pincheira lavas.

Geochemical and petrological data have been critical in developing the authors' understanding of Nevados de Chillán volcano. The results indicate that the volcano has developed two apparently independent magmatic systems located within 6 km of each other. Prior to *ca.* 30 ka, the compositions of lavas do not allow distinction of the two centres. Since 30 ka however, the two subcomplexes have evolved contemporaneously, but independently, with distinctive magma chemistries. Cerro Blanco magmas span a continuous range of $SiO_2$ content, dominantly basaltic andesite to andesite with minor dacite. Las Termas magmas are dominantly low- to high-Si dacite. Considering the proximity of the two centres, it is unlikely that the differences between the two centres are related to differences in primary or parental magma compositions. A control by upper crustal processes is therefore proposed. Magma residence time in the upper crust and magma supply rates are likely to be fundamental controls on the evolutionary behaviour of the systems. The CB system may be replenished and erupt more frequently than the LT system. Again, the perception of the activity of the two centres is liable to be coloured by the much greater detail in which the (much more accessible) LT subcomplex was mapped. The two structures are comparable in volume, but the CB subcomplex is composed of many more individual thin (basaltic) andesite flows than the LT structures. Longer residence times at the LT subcomplex perhaps permit more extensive evolution to high-Si compositions. There may also be unknown local differences in the composition of the upper crustal basement. Differences in local basement structure between the two centres may permit more frequent eruption at CB and could influence magma supply rates from depth within the crust. The paucity of basic to intermediate magmas erupted at LT since the LT3 event may suggest the existence of a large silicic magma body beneath this centre which is inhibiting the passage to the surface of less evolved, more dense magmas.

## CONCLUSIONS

The evolution and volcanic geology of Nevados de Chillán volcano is summarised below.

Subglacial activity at around 2 Ma produced a thick section of hyaloclastite and pillow-breccia which has since been heavily eroded. This activity is unlikely to relate to the present-day Nevados de Chillán volcanic system.

Nevados de Chillán is first recognised as a distinctive volcanic system at around 640 ka with the eruption of thick and extensive subglacial lava flows (Los Pincheira lavas).

The next youngest material dated is andesitic and dacitic lavas between 85 and 68 ka in age. Whether the gap between ~500 ka and ~100 ka material is due to sampling bias or a genuine restriction of output is unclear. The 68.0±1.0 ka age from the Nev1b subglacial dacite is highly precise and confirms glacial ice at 1500 m altitude during Isotope stage 4 of the global ice volume sequence.

Steep, inward-facing arcuate cliffs expose extensive sequences of subaerial lavas to the north-west and south-east of the volcano. These cliffs may be sections of caldera wall (s), but there is no clear evidence to link possible cliff-forming events in the north and south. $^{40}Ar/^{39}Ar$ ages of 81.5±4.0 ka (section base) and 40.9±6.7 ka (mid-way up) have been obtained from the cliffs in the northern and southern sections, respectively.

Extensive Pleistocene ignimbrites were emplaced around 40 ka and the eruptions possibly correlate with caldera formation event(s), producing inward-facing cliffs in the south and northwest.

Two major and independent volcanic centres, the Cerro Blanco (CB) and Las Termas (LT) subcomplexes, developed and are separated by a saddle region with satellite cones and vents. The many vents have a strong NNW-SSE alignment.

At the LT subcomplex, the pre-caldera subaerial lava sequence and caldera collapse were followed by post-caldera dacite lavas with ice-contact features. Interpretation of lava-ice interaction was confirmed by high-precision $^{40}Ar/^{39}Ar$ dating placing eruption early during the last glacial maximum at 30 ka.

In the post-glacial period the LT subcomplex has developed as a complex of overlapping cones from which extensive dacite and silicic-andesite lavas have erupted. Viejo cone has been the source of several moderate-magnitude subplinian and vulcanian explosive eruptions during the Holocene (9,000 to 2,300 BP.). Major historic eruptions (1906-1948 and 1973-1986) constructed steep-sided dacite lava cones.

The CB subcomplex to the north-west consists of an early shield and stratocone complex and associated extensive lavas. This stratocone underwent sector collapse and erosion and a young complex of overlapping cones accumulated upon the remnants. The younger cones contain pyroclastic ejecta and lavas with silicic dacite or andesite compositions.

Moderate magnitude explosive eruptions from the CB subcomplex are indicated by pumice and scoria fall deposits to the east. The most recent eruption occurred in 1861-65 from the satellite Santa Gertrudis vent on the north-west flank. An andesite lava was extruded, melting significant amounts of snow and ice and causing lahars in the Río Santa Gertrudis valley.

The CB and LT subcomplexes have evolved and erupted independently over several thousands of years despite their centres being only 6-8 km apart. The CB3b Los Baños cone and LT5c Shangri-La dome in the saddle between the subcomplexes are less than 500 m apart, yet are geochemically distinct.

Holocene pyroclastic flow deposits are found in the valleys around the volcano. Radiocarbon ages indicate, at least, three different eruptions. The flow deposits are highly weathered, fine-grained and andesitic.

Lahars due to melting of snow and ice have been recorded in the historic past and may be expected to be a hazard during future eruptions (especially during winter).

## ACKNOWLEDGEMENTS

This study was supported by the Overseas Development Administration (now DFID) under Project R5563, Volcanic Hazard Mapping for Development Planning, part of the Technical Development and Research (TDR) programme. RSJS acknowledges support from the Leverhulme Trust (ref. 180/SAL) and a NERC professorship. HJD was supported by NERC studentship GT4/95/28E. JAN acknowledges FONDECYT Project 1960186 (Postglacial explosive volcanism).

## REFERENCES

Bacon, C.R. 1986. Magmatic inclusions in silicic and intermediate volcanic rocks. *Journal of Geophysical Research - Solid Earth and Planets*, Vol. 91, (B6), p. 6091-6112.

Blundy, J.S.; Sparks, R.S.J. 1992. Petrogenesis of mafic inclusions in granitoids of the Adamello Massif. *Journal of Petrology*, Vol. 104 p. 208-214.

Déruelle, B. 1977. Sur l' activité recente des Nevados de Chillán (Chili Central). *Comptes Rendus de l' Academie des Sciences de Paris*, Vol. 284 (D), p. 1651-1654.

Déruelle, B.; Déruelle, J. 1974. Los volcanes Cuaternarios de los Nevados de Chillán (Chile central) y reseña sobre el volcanismo Cuaternario de los Andes Chilenos. *Estudios Geológicos*, Vol. 30, p. 91-108.

Ferguson, K.M.; Dungan, M.A.; Davidson, J.P.; Colucci, M.T. 1992. The Tatara-San Pedro Volcano, 36°S,

Chile: a chemically variable, dominantly mafic magmatic system. *Journal of Petrology*, Vol. 33, p. 1-43.

Furnes, H.; Fridleifsson, I.B.; Atkins, F.B. 1980. Subglacial volcanics - on the formation of acid hyaloclastites. *Journal of Volcanology and Geothermal Research*, Vol. 8, p. 95-110.

Gajardo, A. 1981. Hoja Concepción-Chillán, Región del Bio-Bío. *Instituto de Investigaciones Geológicas, Mapas Geológicos Preliminares de Chile*, No. 4, escala 1:250.000.

Gill, J.B. 1981. Orogenic Andesites and Plate Tectonics. *Springer-Verlag*, 390 p. Berlin.

Jones, J.G. 1969. Intraglacial volcanoes of the Laugarvatn region, southwest Iceland. *Geological Society of London Quarterly Journal*, Vol. 124, p. 197-211.

Lescinsky, D.T.; Sisson, T.W. 1998. Ridge-forming, ice-bounded lava flows at Mount Rainier, Washington. *Geology*, Vol. 26, No. 4, p. 351-354.

Muñoz, J.; Niemeyer, R. 1984. Hoja Laguna del Maule, Regiones del Maule y del Bio-Bío. *Servicio Nacional de Geología y Minería, Carta Geológica de Chile*, No. 64, escala 1:250.000.

Naranjo, J.A.; Chávez, R.; Sparks, R.S.J.; Gilbert, J.; Dunkley, P.N. 1994. Nuevos antecedentes sobre la evolución Cuaternaria del Complejo Volcánico Nevados de Chillán. *In Congreso Geológico Chileno, No. 7, Actas*, Vol. 1, p. 342-345. Concepción.

Sigvaldason, G.E. 1968. Structure and products of subaquatic volcanoes in Iceland. *Contributions to Mineralogy and Petrology*, Vol. 18, p. 1-16.

Singer, B.S.; Pringle, M.S. 1996. Age and duration of the Matuyama-Brunhes geomagnetic polarity reversal from $^{40}Ar/^{39}Ar$ incremental heating analyses of lavas. *Earth and Planetary Science Letters*, Vol. 139, p. 47-61.

Singer, B.S.; Thompson, R.A.; Dungan, M.A.; Feeley, T.C.; Nelson. S.T.; Pickens, J.C.; Brown, L.L.; Wulff, A.W.; Davidson, J.P.; Metzger, J. 1997. Volcanism and erosion during the past 930 k.y. at the Tatara-San Pedro complex, Chilean Andes. *Geological Society of America, Bulletin*, Vol. 109, No. 2, p. 127-142.

Smellie, J.L.; Hole, M.J.; Nell, P.A.R. 1993. Late Miocene valley-confined subglacial volcanism in Northern Alexander Island, Antarctic Peninsula. *Bulletin of Volcanology*, Vol. 55, No. 4, p. 273-288.

Smellie, J.L.; Millar, I.L.; Rex, D.C.; Butterworth, P.J. 1998. Subaqueous, basaltic lava dome and carapace breccia on King George Island, South Shetland Islands, Antarctica. *Bulletin of Volcanology*, Vol. 59, No. 4, p. 245-261.

Tormey, D.R.; Frey, F.A.; López-Escobar, L. 1995. Geochemistry of the active Azufre-Planchón-Peteroa volcanic complex, Chile (35°15'S) - evidence for multiple sources and processes in a cordilleran arc magmatic system. *Journal of Petrology*, Vol. 36, No. 2, p. 265-298.

Walker, G.P.L. 1973. Explosive volcanic eruptions: A new classification scheme. *Geologische Rundschau*, Vol. 62, p. 431-436.

Walker, G.P.L.; Blake, D.H. 1966. The formation of a palagonite breccia mass beneath a valley glacier in Iceland. *Quarterly Journal of the Geological Society of London*, Vol. 122, p. 45-61.

Werner, R.; Schmincke, H.U.; Sigvaldason, G. 1996. A new model for the evolution of table mountains - volcanological and petrological evidence from Herdubreid and Herdubreidartögl volcanos (Iceland). *Geologische Rundschau*, Vol. 85, No. 2, p. 390-397.

Manuscript received: November 24, 1998; accepted: September 21, 1999.